

Near Real Time Ultra High Resolutions ASCAT Wind Vector and Ice Products in US Coastal Zones

Seubson “Golf” Soisuvarn, Zorana Jelenak, Qi Zhu, Casey Shoup, Joe Sapp, and Paul S. Chang

NESDIS/STAR/Ocean Surface Winds Team

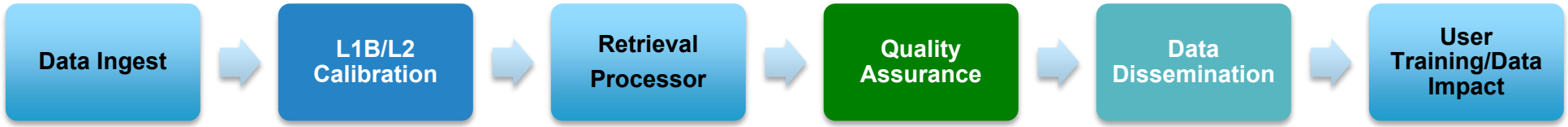
National Environmental Satellite, Data, and Information Service

NOAA CoastWatch Seminar
February 13, 2025, Virtual Meeting

The views, opinions, and findings in this report are those of the authors and should not be construed as an official NOAA or U.S. government position or policy.

Ocean Winds Science Team Data Processing System (OWTDPS)

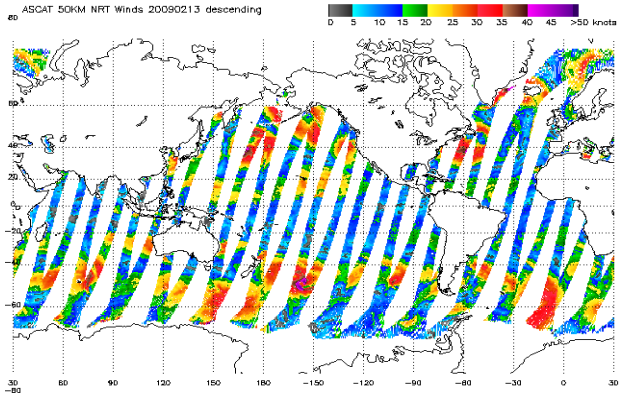
- This processing system consists of six major components: data ingesting, calibration-validation, retrieval algorithm, product and data monitoring, data dissemination via web/data portal and user training and data impact assessment

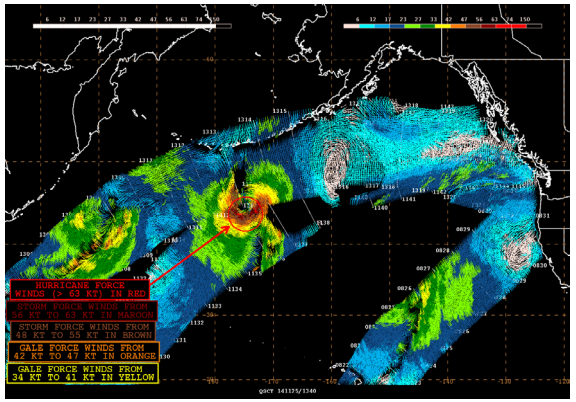


ASCAT B/C (9 Products)
OSCAT-3 (9 Products)
ASMR-2 (22 products)
SMAP (1 Product)
CYGNSS (1 Product)
Aircraft IWRAP/KaIA (12 Products)
COWVR – in CAL/VAL

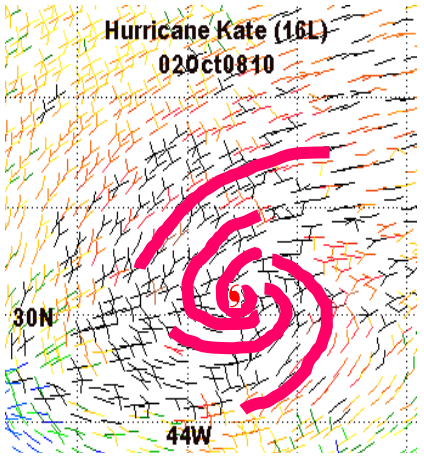
Currently processed in NRT in OWTDPS
Producing total of 56 Products

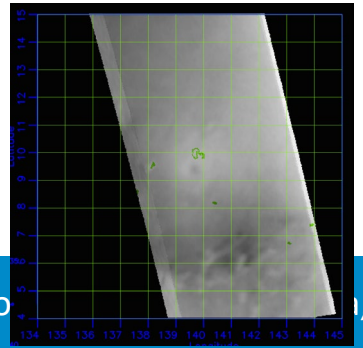
STAR Full Suite of Scatterometry Products

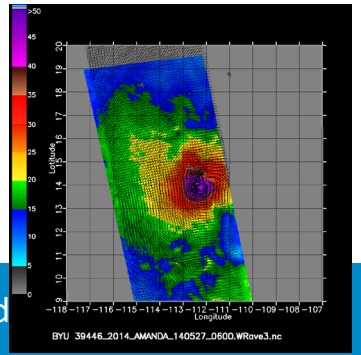


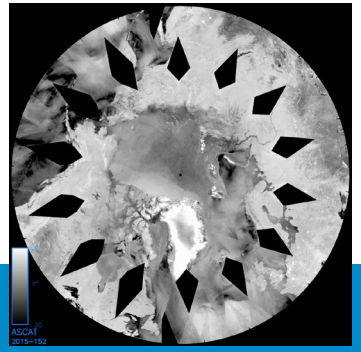


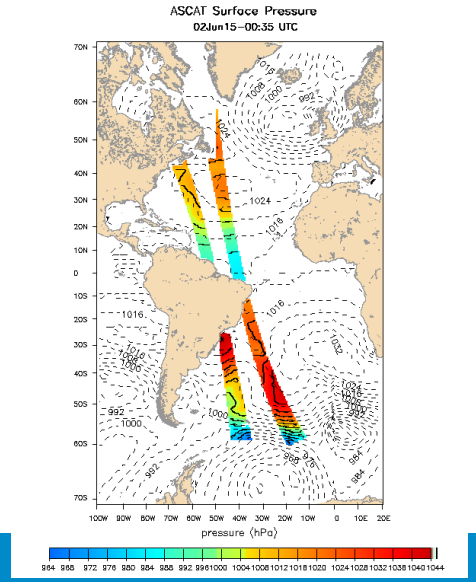
- **Low and high resolution global**
  - Scatterometer wind vectors
  - Wind vector ambiguities
- **NAWIPS and AWIPS ready** wind vector products for NWS operations
- **BUFR ready** wind vector products for Data Assimilation
- **Ultra high resolutions NRCS imagery** for
  - TC positioning
  - Oil spill detections
- **Ultra high resolution TC** wind vector product
- **Ultra high resolution coastal and ice**
- Scatterometer derived sea **surface pressure fields**
- **Ice products**











https://manati.star.nesdis.noaa.gov/datasets/AscatCoastalUHR.php

STAR Center for Satellite Applications and Research
National Environmental Satellite, Data, and Information Service (NESDIS)
Ocean Surface Winds Team

NOAA | NESDIS | STAR | SOCD
OSWT Home | Product Description | Data Products | Research | Contact Us

Select a Date to Display UHR ASCAT Coastal Images

02/12/2025

Prev Day | Next Day

Today | Latest

- OSWT Home
- Product Description
- Current Data Products
  - Aircraft Data
  - Alaska ASCAT Coastal Products
  - Altimeter
  - Animated ASCAT Ice Products
  - ASCAT (METOP-B)
  - ASCAT (METOP-C)
  - ASCAT Coastal UHR >>
  - CYGNSS
  - GCOMW1/AMSR2
  - OSCAT-3
  - Satellite Prediction
  - SMAP
- Past Data Products
  - ASCAT (METOP-A)
  - ERS-2
  - OSCAT
  - QuikSCAT/SeaWinds
  - RapidSCAT
  - SCATSAT
  - SSM/I
  - WindSAT
- Research
- Contact Us

Enter search term(s) Go
This site only All of NOAA
Advanced Search

Click the coastal zone to view images for that coastline/region

Ice Sigma0 available for Alaska and Great Lakes regions when applicable.

Current Zone Selected: Gulf Coast

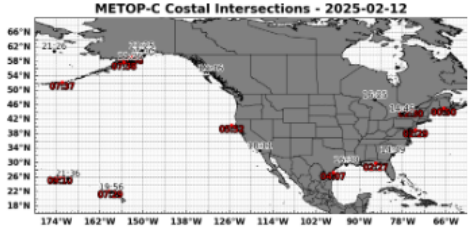


Estimated Coastal Intersections

METOP-B Costal Intersections - 2025-02-12



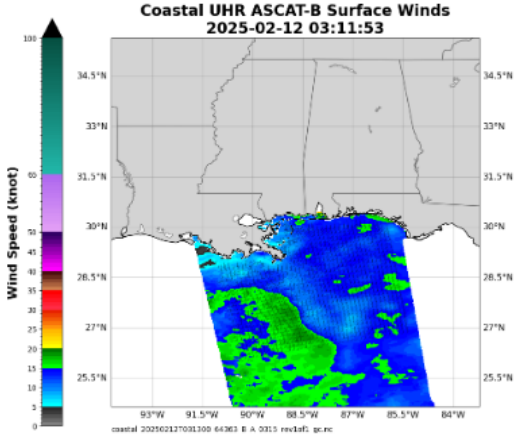
METOP-C Costal Intersections - 2025-02-12



Notes (click to expand)

ASCAT-B - Ascending

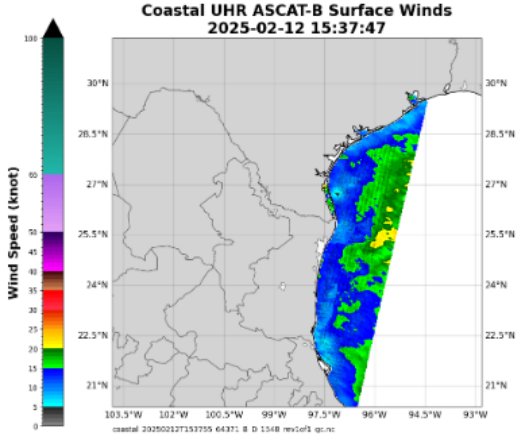
1 image(s)



Sigma0 image netcdf file

ASCAT-B - Descending

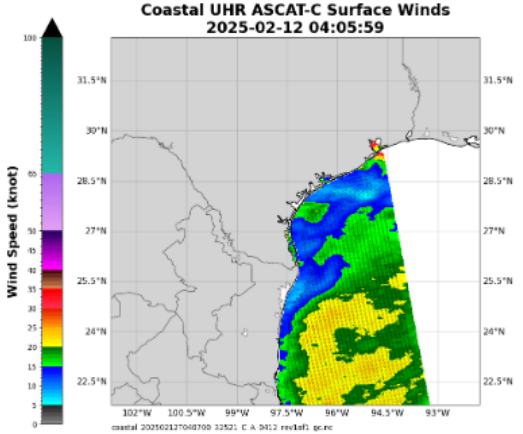
1 image(s)



Sigma0 image netcdf file

ASCAT-C - Ascending

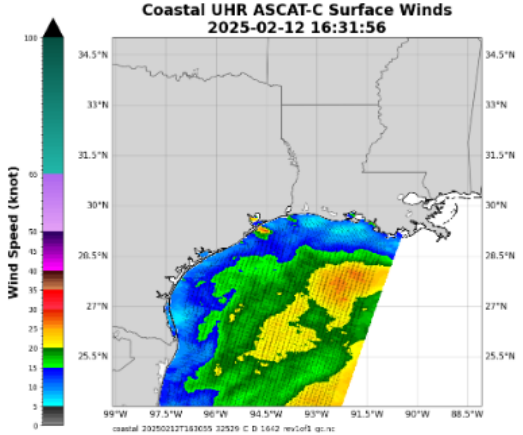
1 image(s)



Sigma0 image netcdf file

ASCAT-C - Descending

1 image(s)



Sigma0 image netcdf file

STAR Center for Satellite Applications and Research

National Environmental Satellite, Data, and Information Service (NESDIS)

Ocean Surface Winds Team

https://manati.star.nesdis.noaa.gov/datasets/AlaskaASCATCoastal.php

NOAA | NESDIS | STAR | SOCD

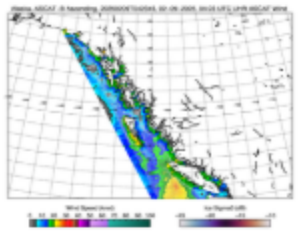
OSWT Home | Product Description | Data Products | Research | Contact Us

- OSWT Home
- Product Description
- Current Data Products
  - Aircraft Data
  - Alaska ASCAT Coastal Products
  - Altimeter
  - Animated ASCAT Ice Products
  - ASCAT (METOP-B)
  - ASCAT (METOP-C)
  - ASCAT Coastal UHR
  - CYGNSS
  - GCOMW1/AMSR2
  - OSCAT-3
  - Satellite Prediction
  - SMAP
- Past Data Products
  - ASCAT (METOP-A)
  - ERS-2
  - OSCAT
  - QuikSCAT/SeaWinds
  - RapidSCAT
  - SCATSAT
  - SSM/I
  - WindSAT
- Research
- Contact Us

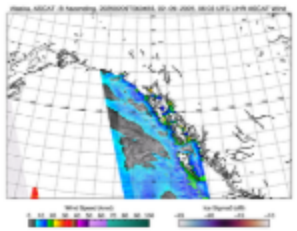
Data from Satellite/Instruments: Alaska ASCAT Coastal Products

Additional Products: Alaska ASCAT-B Coastal prod | Year: 2025 | Month: 2 | Day: 9 | Get Images

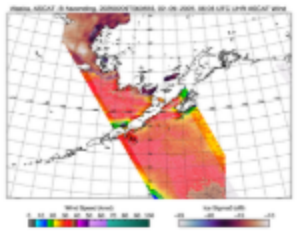
Alaska ASCAT-B Coastal Products



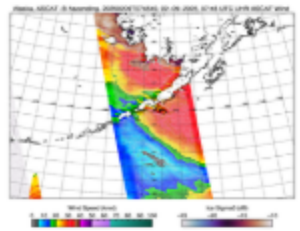
ASCAT-B UHR Speed
02/09/25 04:23 UTC



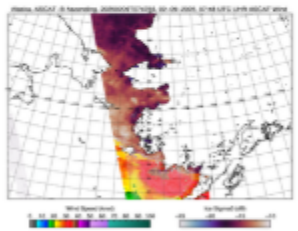
ASCAT-B UHR Speed
02/09/25 06:03 UTC



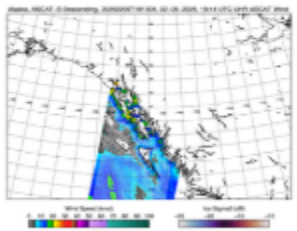
ASCAT-B UHR Speed
02/09/25 06:05 UTC



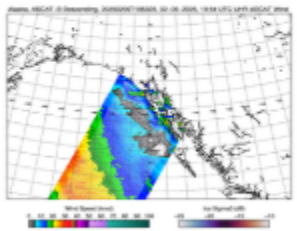
ASCAT-B UHR Speed
02/09/25 07:45 UTC



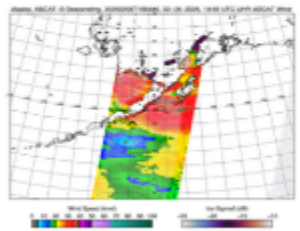
ASCAT-B UHR Speed
02/09/25 07:48 UTC



ASCAT-B UHR Speed
02/09/25 18:14 UTC



ASCAT-B UHR Speed
02/09/25 19:54 UTC

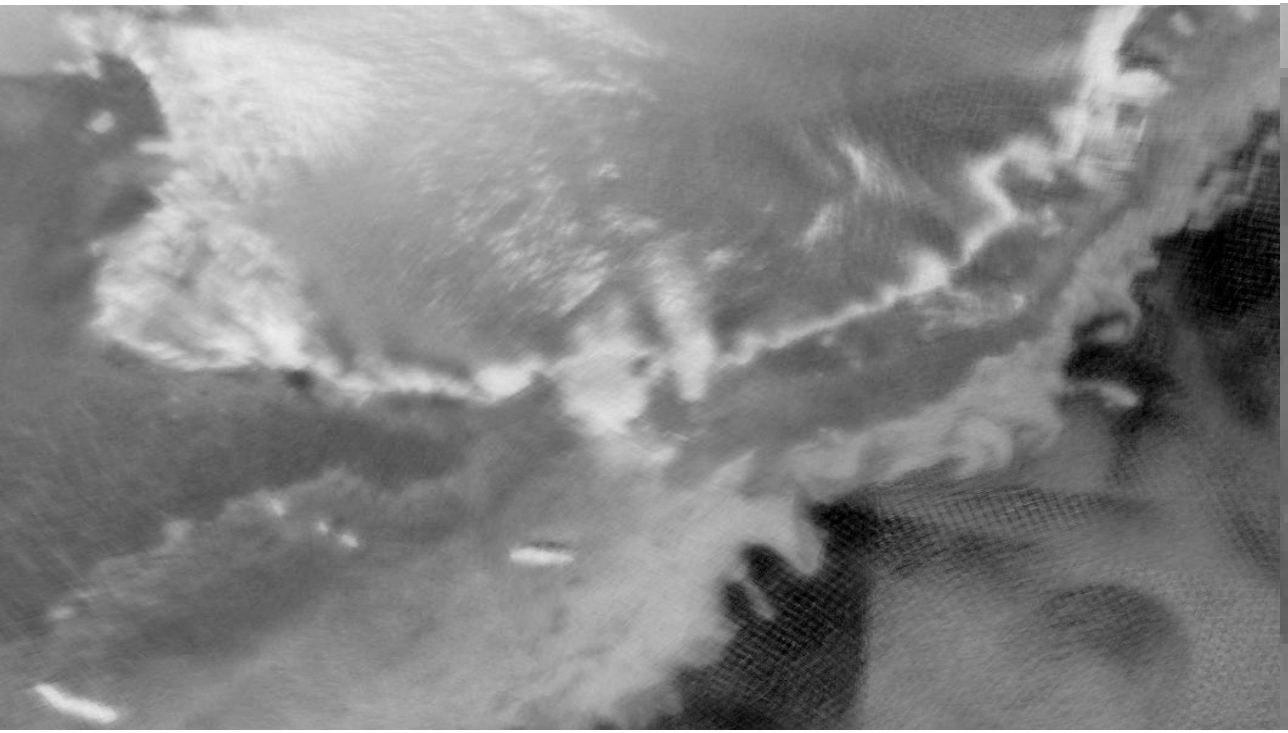


ASCAT-B UHR Speed
02/09/25 19:55 UTC

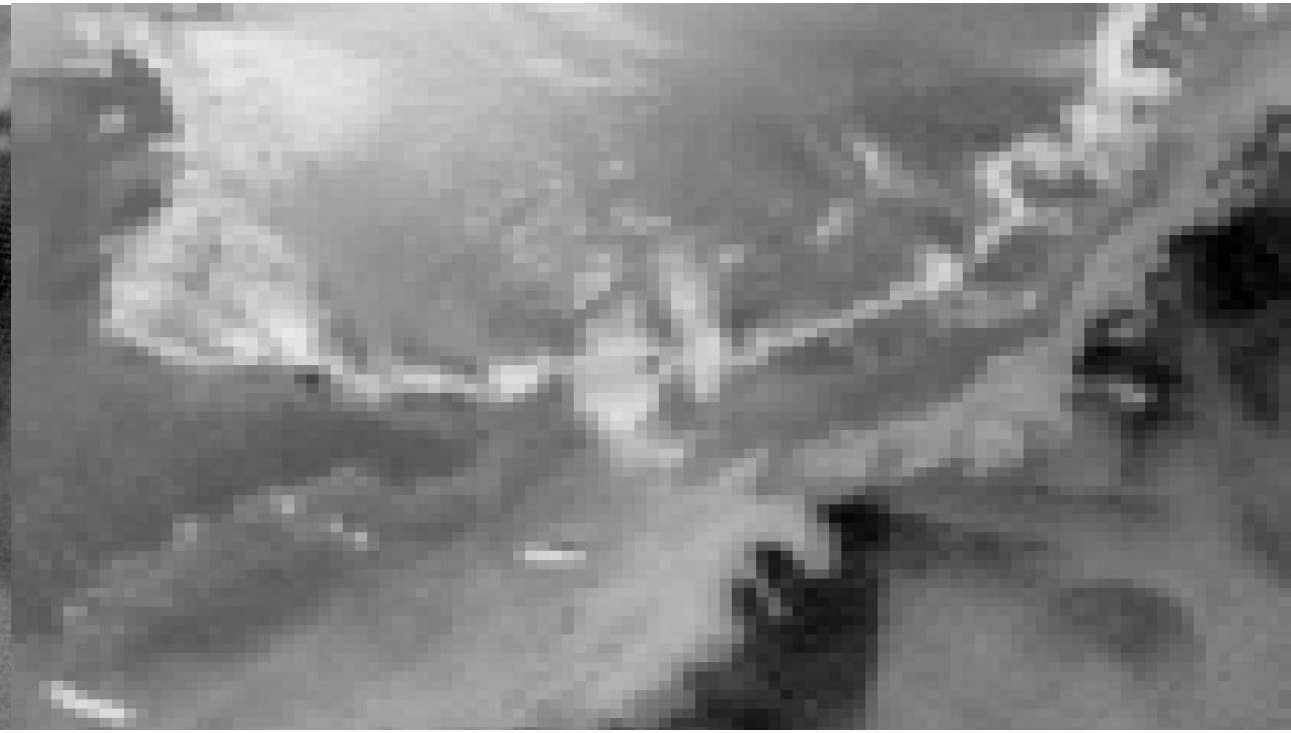
Introduction

- Ultra High Resolution (UHR) scatterometer processing techniques has been developed by Professor David Long of BYU.
- NESDIS/STAR Ocean Surface Wind Team (OSWT) has demonstrated a coastal feasibility utilizing the UHR processing for SCATSAT-1 and later for ASCAT.
- The UHR ASCAT coastal products has been generating routinely in near real-time (NRT) for
  - Tropical cyclone specific UHR ASCAT products.
  - US coastal regions

Scatterometer Spatial Resolution Enhancement
(BYU's David Long)



AVE (2.225 km pixels)

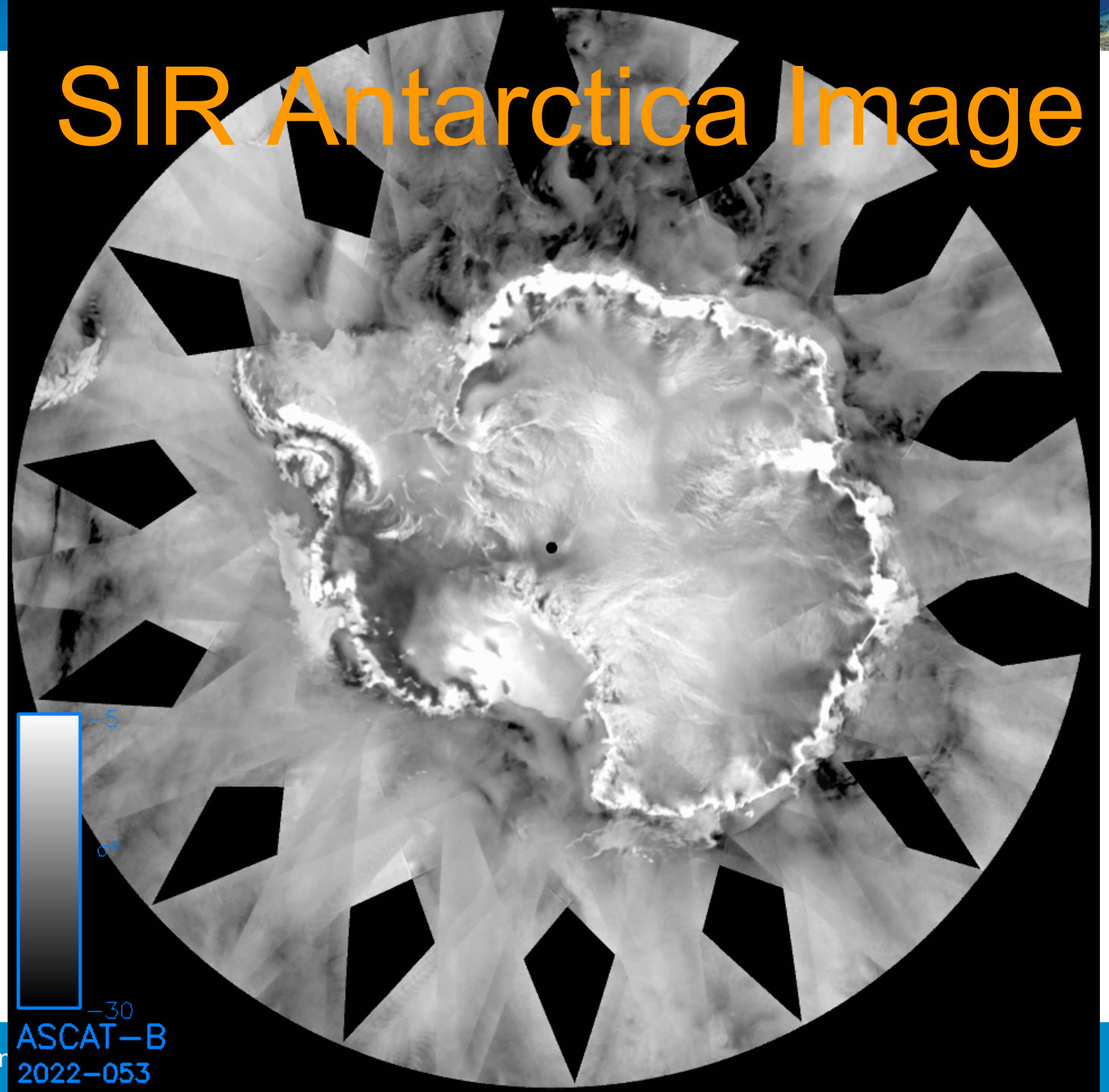


25 km gridded (grd)

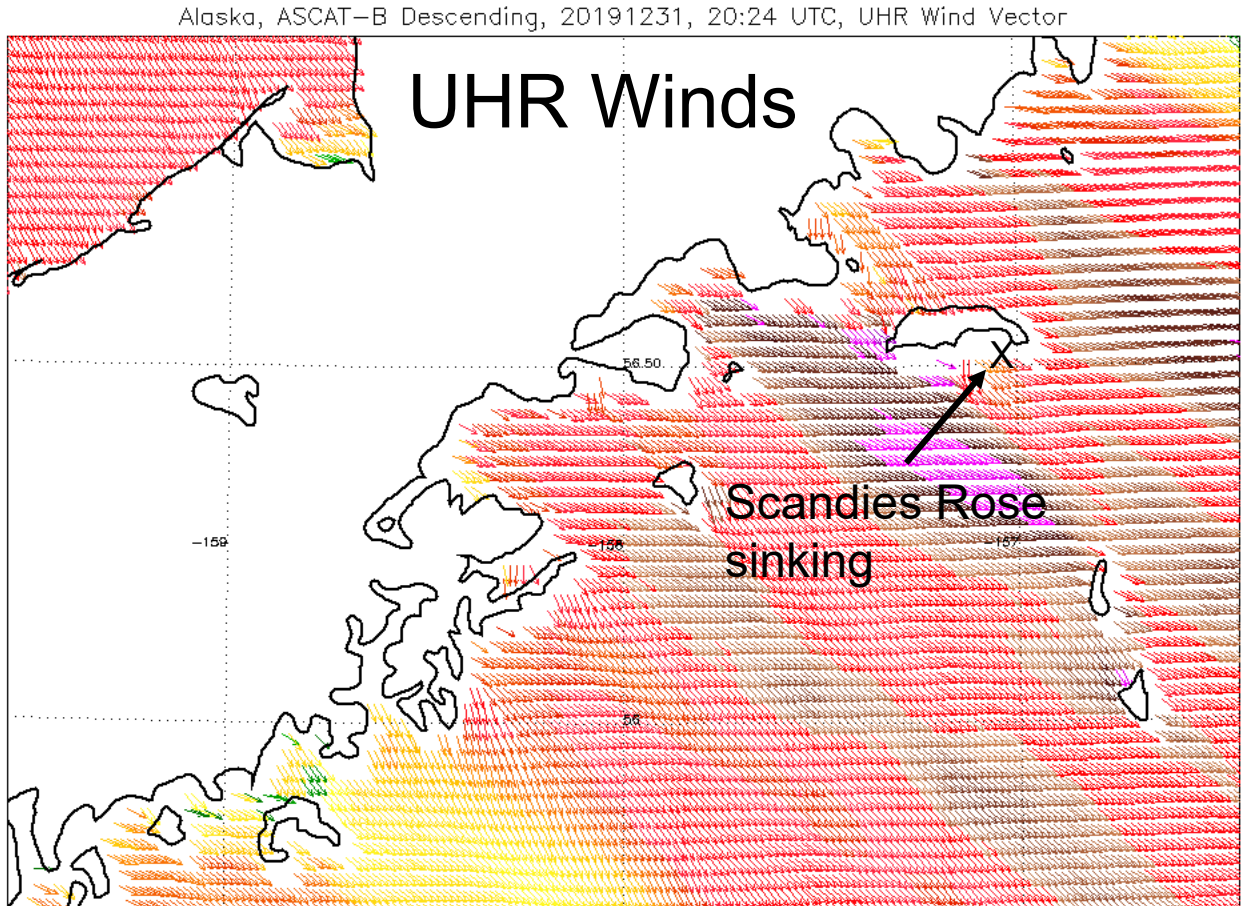
Enhanced Resolution Techniques

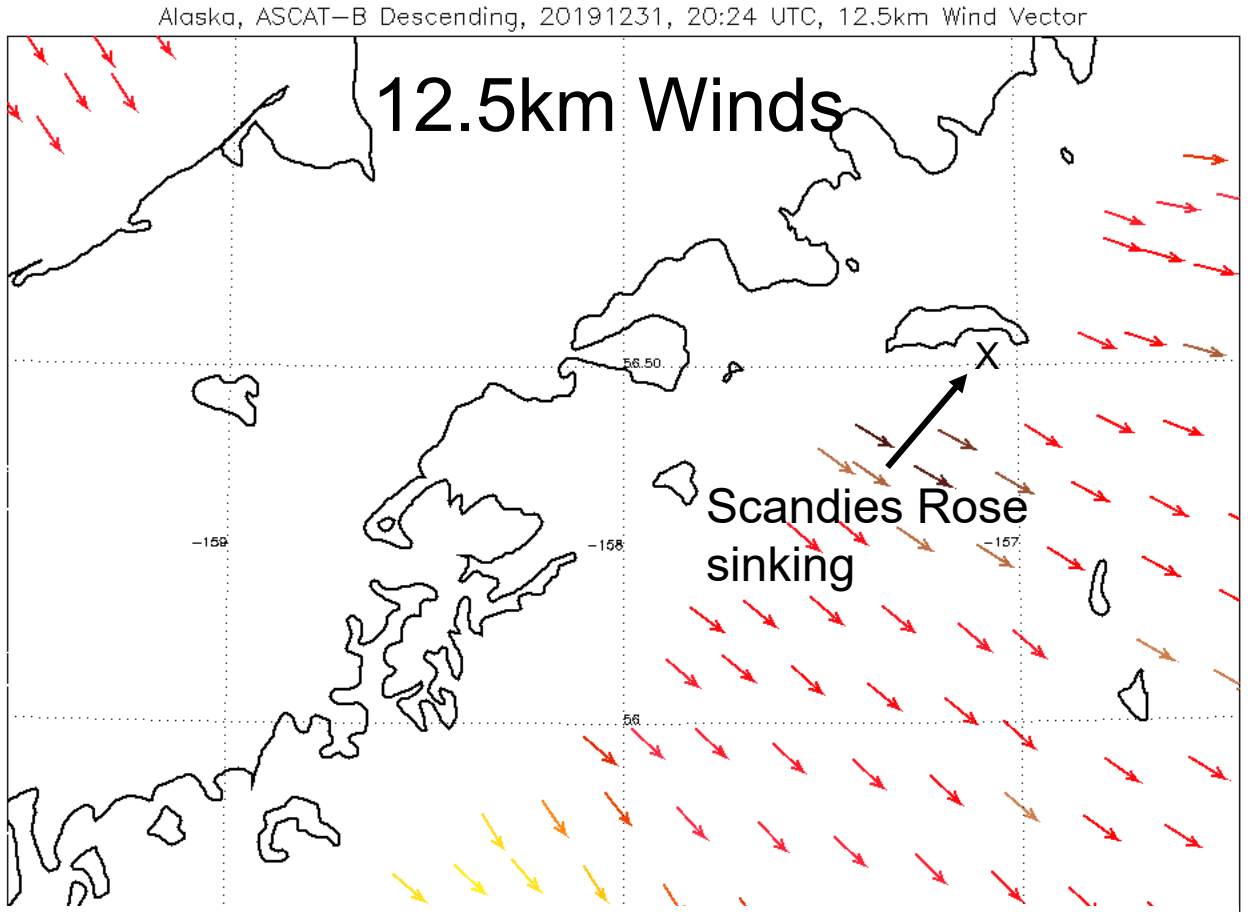
- Scatterometer Image Reconstruction (SIR)
  - Required multiple observation passes
  - Lost temporal information
  - Can create much higher resolution than a single pass observation
  - Suitable for land and ice imagery applications
  - SIR Image is independent of the incidence angle (typical normalized to 40 deg)
- Weighted AVErage (AVE)
  - Only 1 observation pass is enough for sigma0 sampling
  - Preserve measurement geometry information
    - Incidence angle, azimuth angle
  - Suitable for high resolution wind retrieval application

SIR Antarctica Image



Scandies Rose sinking 2019





The National Transportation Safety Board said the vessel's inaccurate stability instructions combined with heavy lopsided ice accumulation due to wind and sea conditions, which were more extreme than forecasted during the voyage, caused the vessel to sink near Sutwik Island.

Ultra High Resolution (UHR) Sigma0 Processing

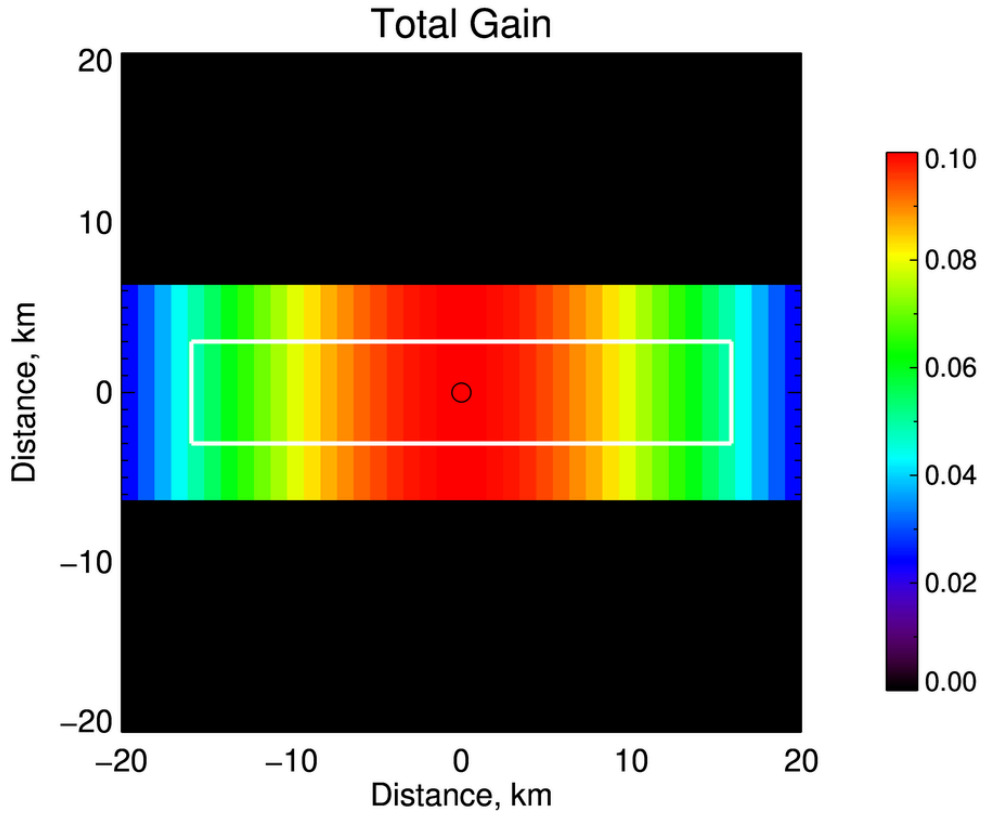
- Sigma0 slices can be expressed as:

$$\sigma_i^0 = \sum_{j=1}^{n} h_{ij}\sigma_{ij}^0 \qquad (1)$$

where h_{ij} and σ^0_{ij} is the weighted Spatial Response Function (SRF) and surface sigma0 respectively from the i^{th} measurement and the j^{th} pixel.

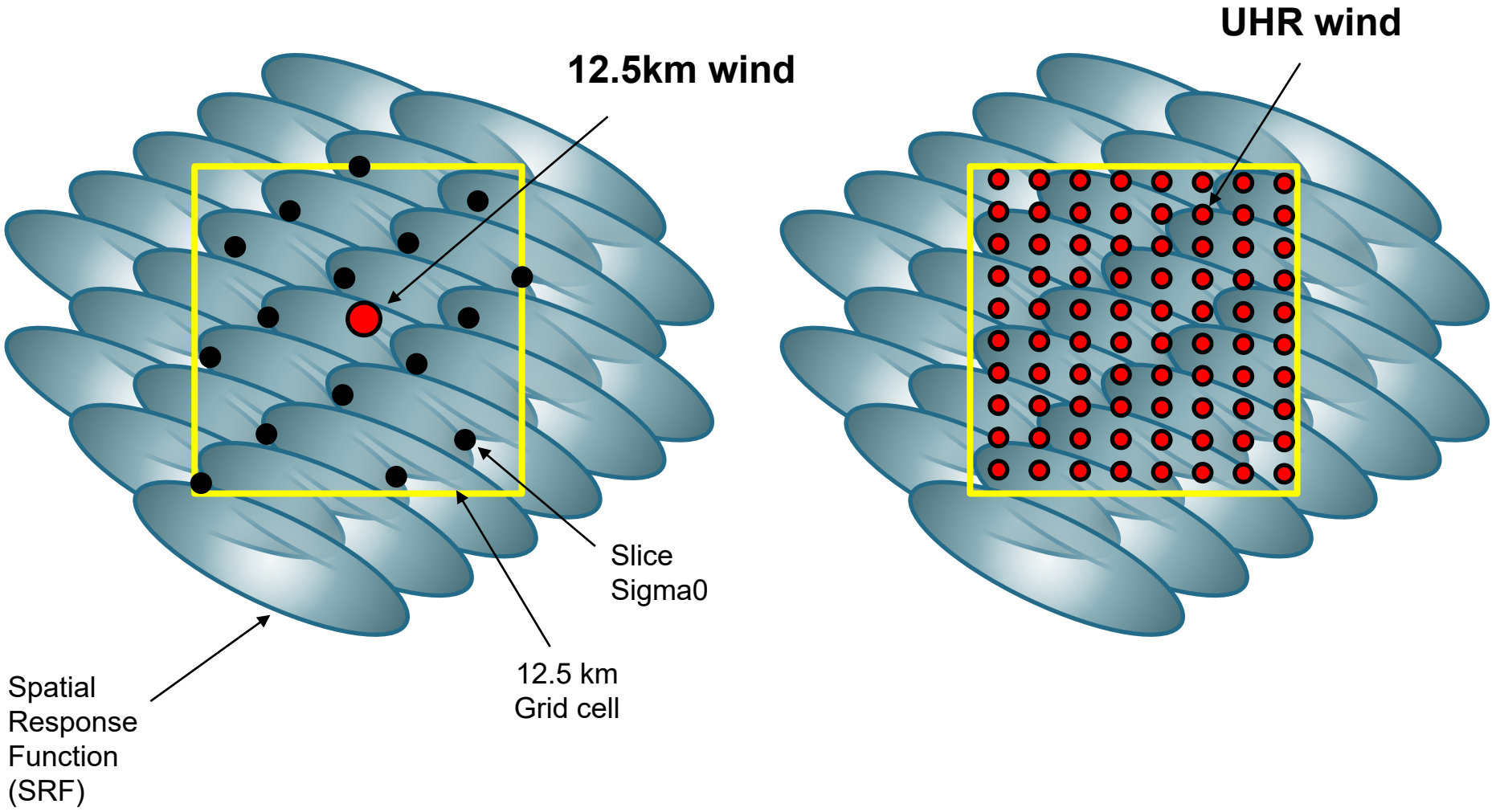
- The UHR sigma0 can produced using the BYU's Average (AVE) algorithm:

$$\sigma^0_{ave,j} = \frac{\sum_i \sigma_i^0 h_{ij}}{\sum_i h_{ij}} \qquad (2)$$

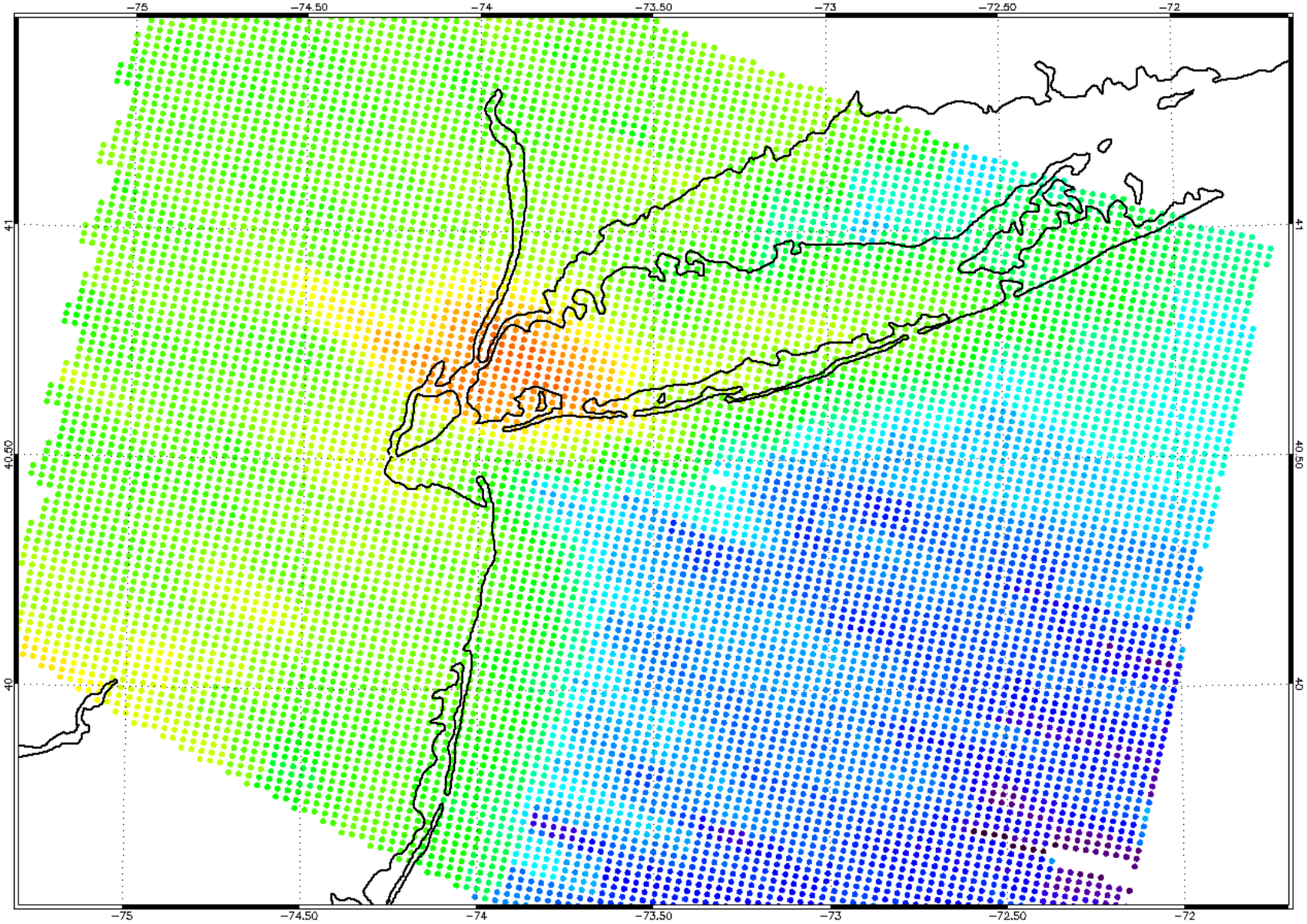


Spatial Response Function (SRF) example

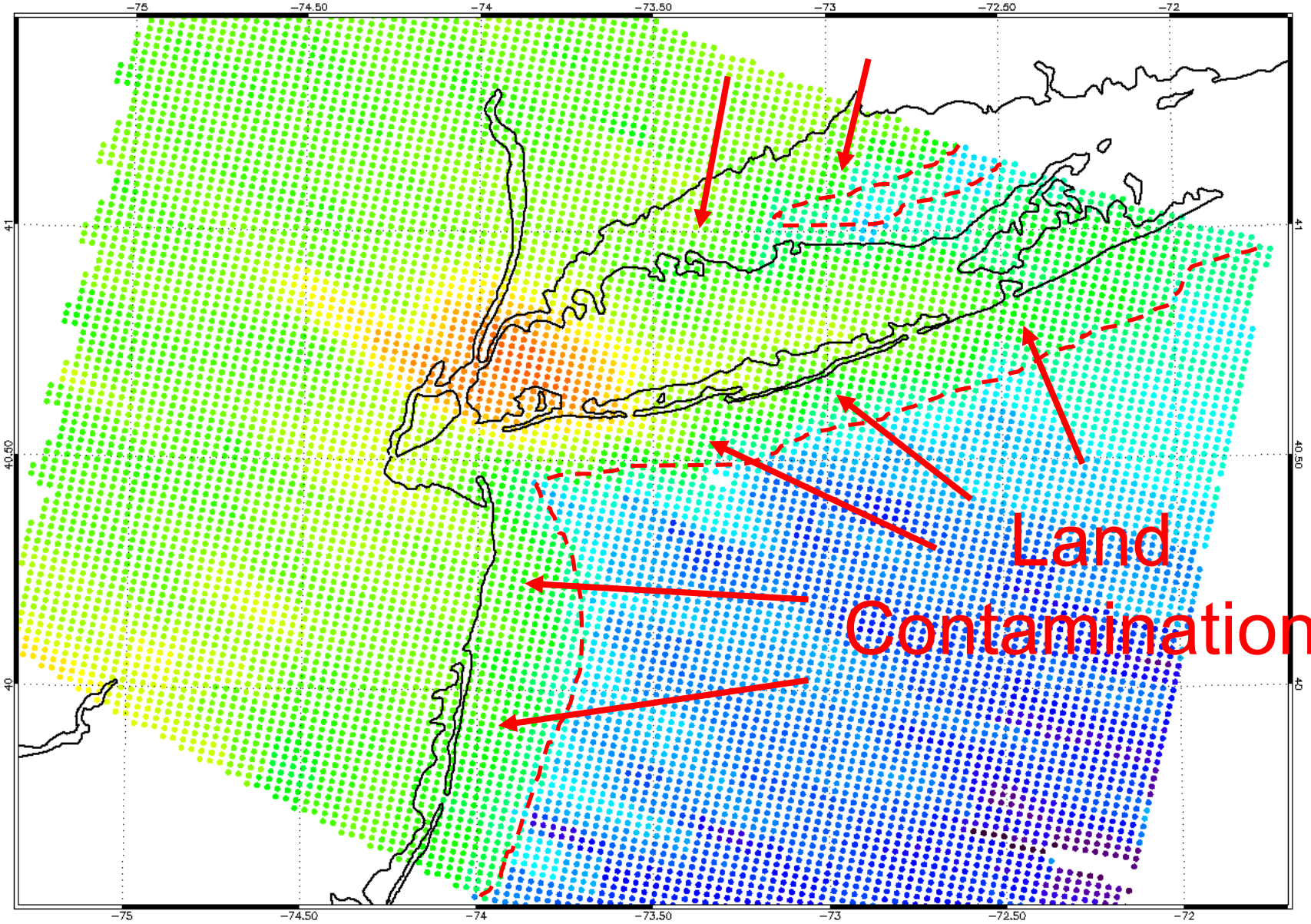
Standard vs UHR Sigma0 Gridding



UHR Sigma0



UHR Sigma0



Land Contamination Correction

- Sigma0 slice can be expressed as a summation of land-only and ocean-only sigma0 as

$$\sigma_i^0 = \sigma_{Land}^0 + \sigma_{Ocean}^0 \qquad (3)$$

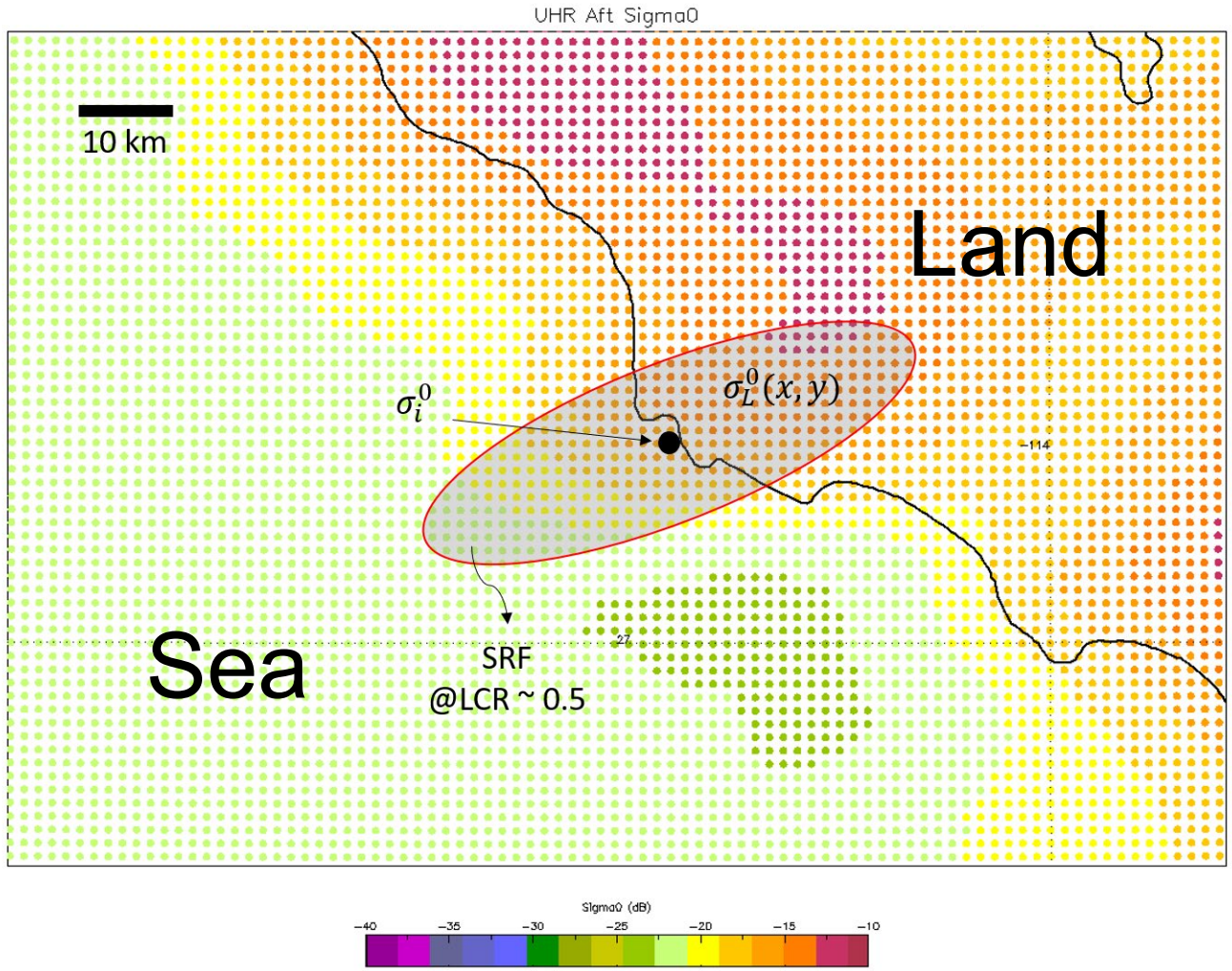
- The land-only signal can be expanded into

$$\sigma_{Land}^0 = \frac{\sum \sigma_L^0(x,y) \cdot G_L(x,y)}{\sum G_L(x,y)} \cdot LCR \qquad (4)$$

where the $\sigma^0_L(x,y)$ is the surface sigma0 over land and the $G_L(x,y)$ is the gain response portion over land. LCR is the land contribution ratio.

- The summation ratio in (4) is defined a weighted average land sigma0 as

$$\sigma_{L,ave}^0 = \frac{\sum \sigma_L^0(x,y) \cdot G_L(x,y)}{\sum G_L(x,y)} \qquad (5)$$



Land Contamination Correction – cont.

- The initial land contaminated sigma0 can be corrected as

$$\sigma^0_{Ocean} = \sigma^0_i - \sigma^0_{L,ave} \cdot LCR \qquad (6)$$

- To incorporate land standard deviation $\sigma^0_{L,std}$, (6) is modified through iteration process by

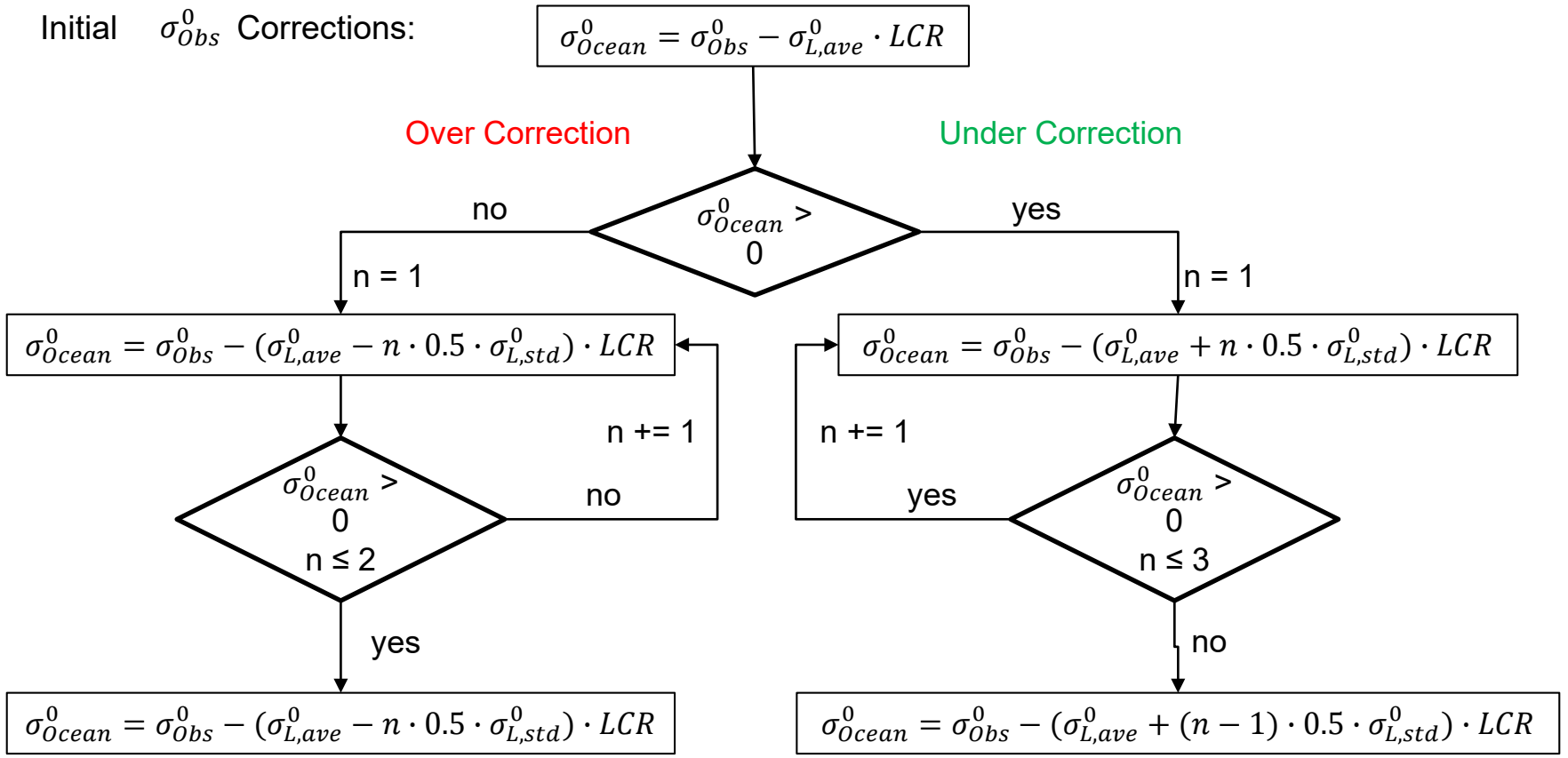
$$\sigma^0_{Ocean} = \sigma^0_i - (\sigma^0_{L,ave} \pm n \cdot 0.5 \cdot \sigma^0_{L,std}) \cdot LCR \qquad (7)$$

- Finally, the AVE algorithm can be modified as

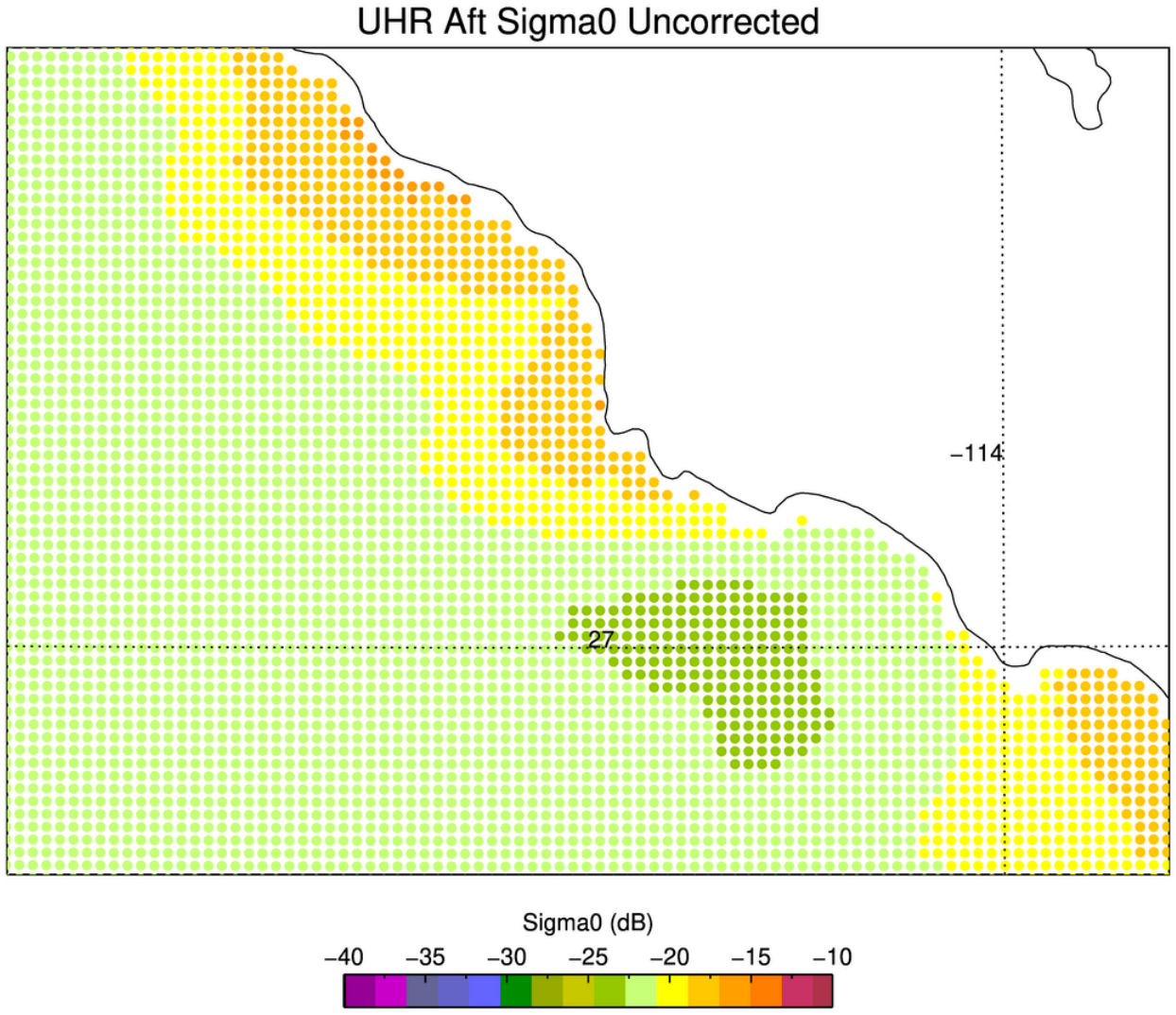
$$\sigma^0_{ave,j} = \frac{\sum_i \sigma^0_{Ocean} h_{ij}}{\sum_i h_{ij}} \qquad (8)$$

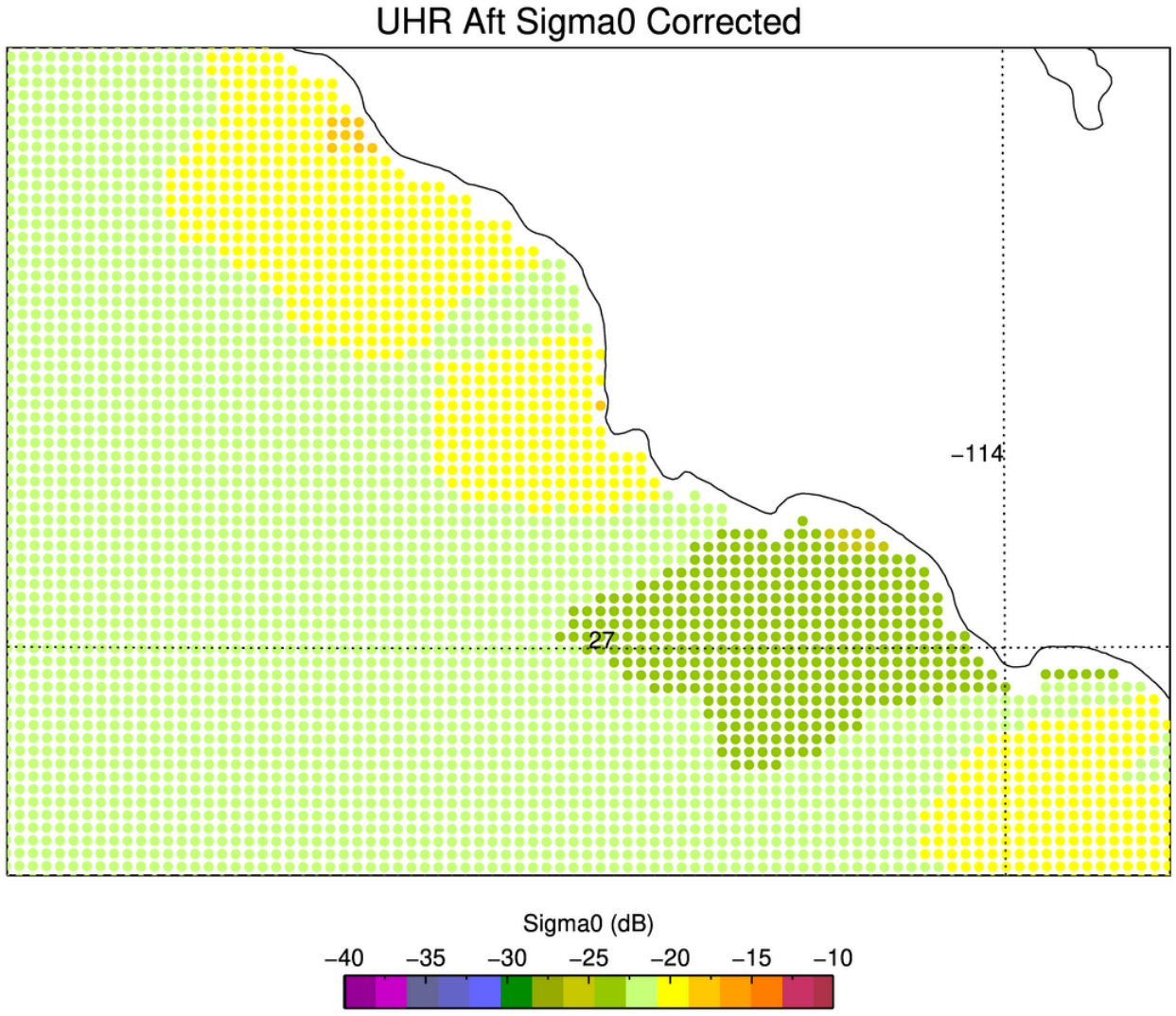
Land Contamination Correction – cont.

Initial σ^0_{Obs} Corrections:



Case Study #1



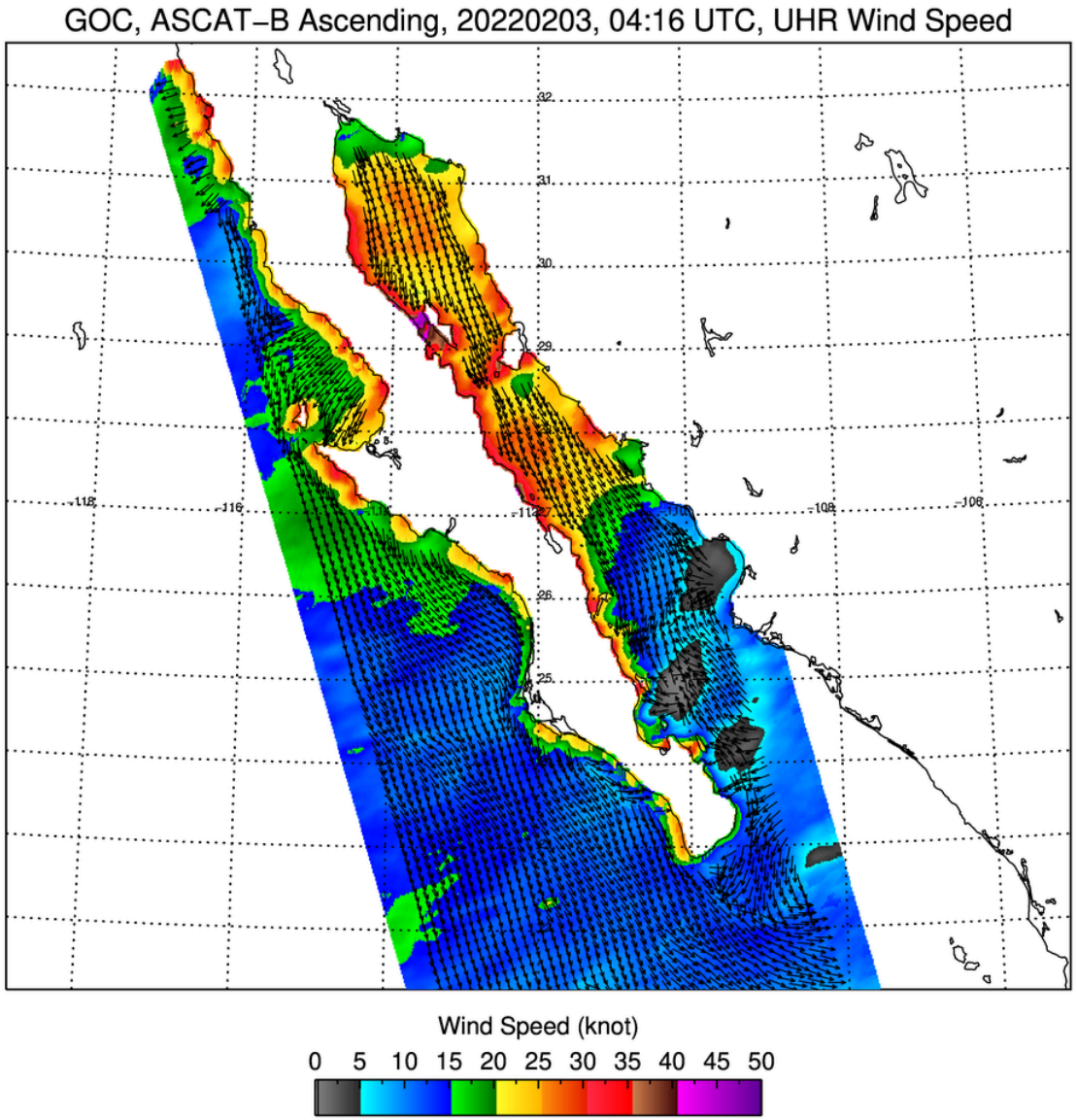


σ^0_{ave} using uncorrected σ^0_i

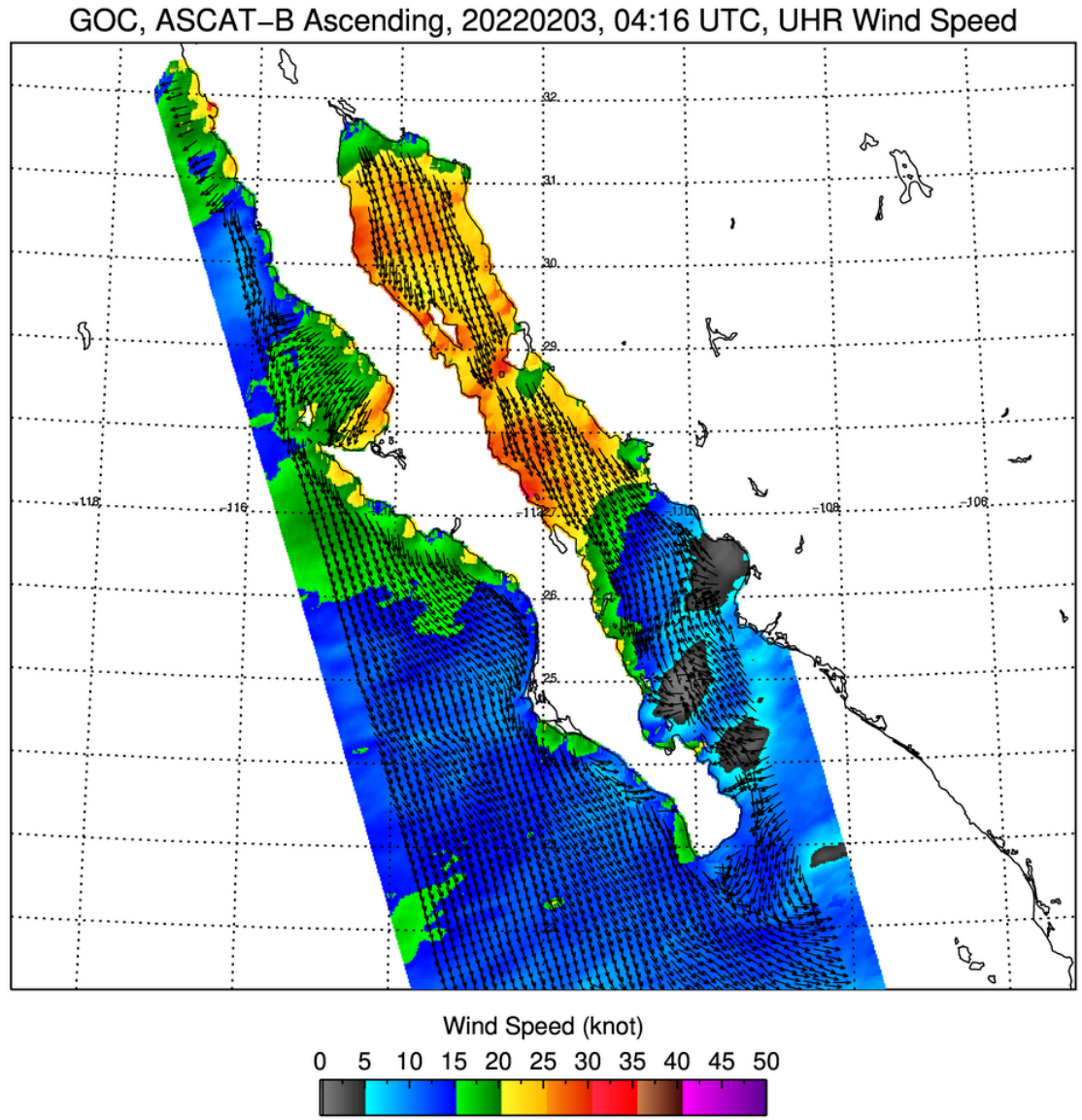
LCR Threshold = 0.5

σ^0_{ave} using corrected σ^0_i

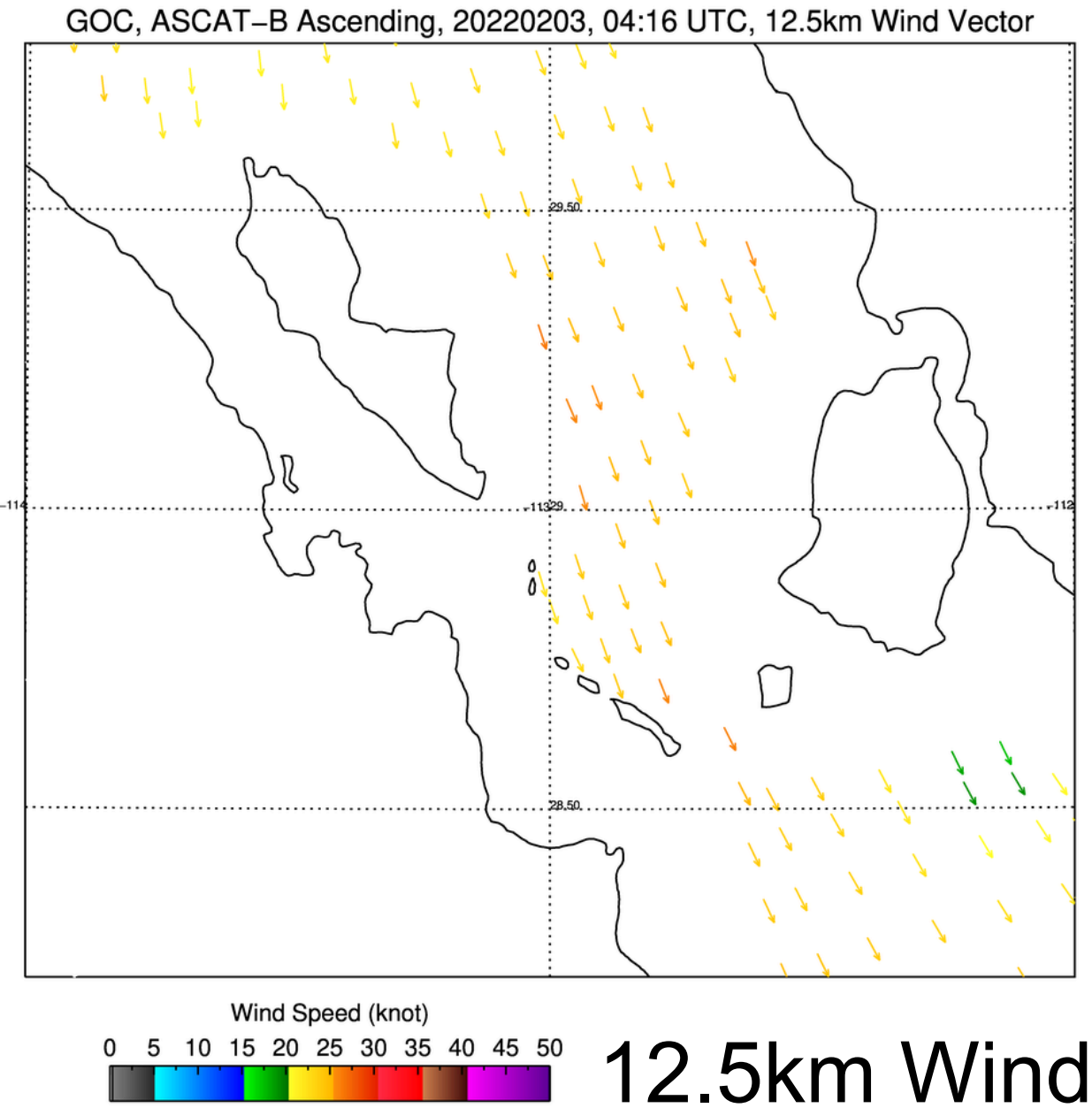
LCR Threshold = 0.5



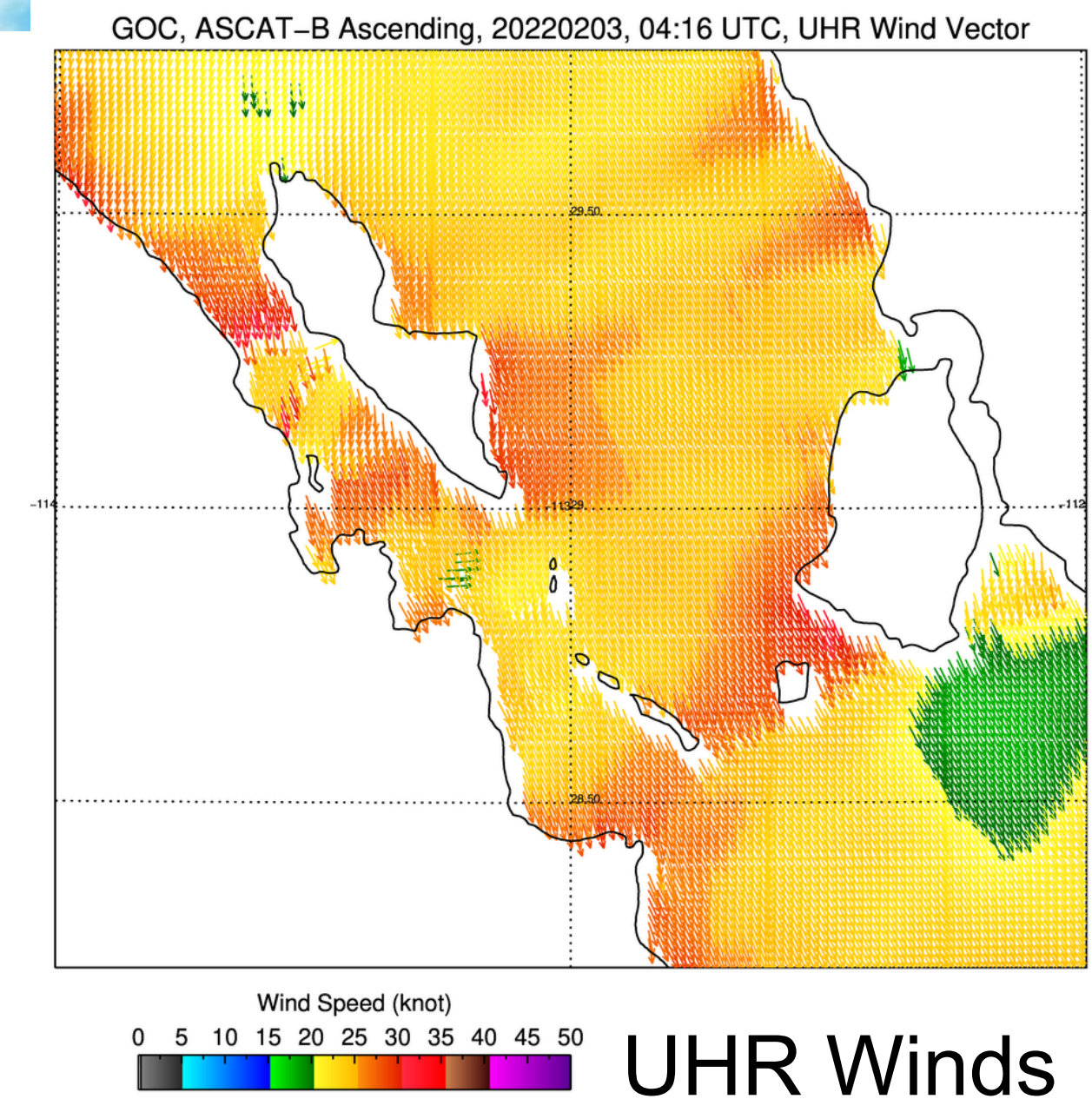
High-Resolution Processing
Without Land Contamination Correction



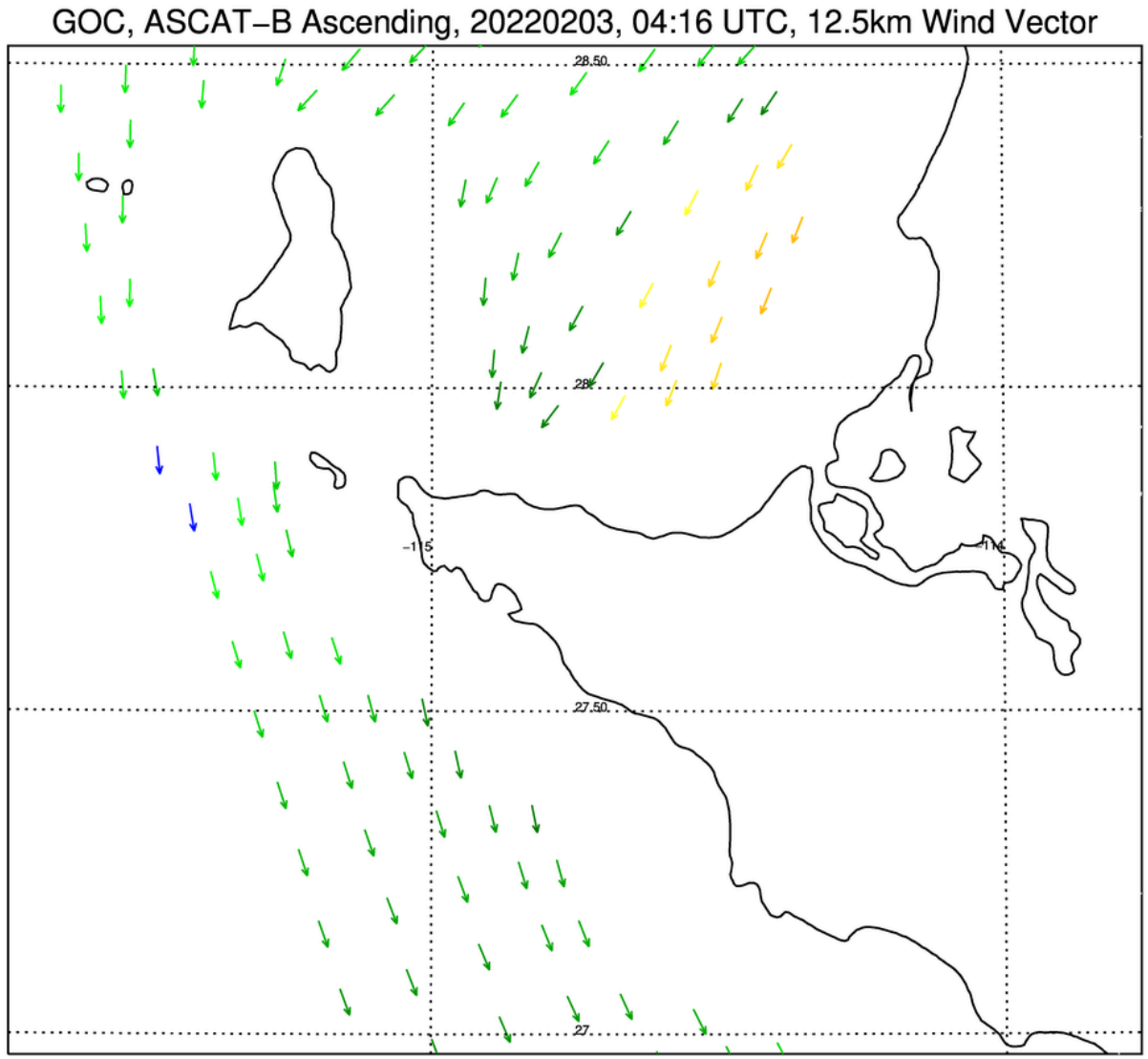
High-Resolution Processing
With Land Contamination Correction



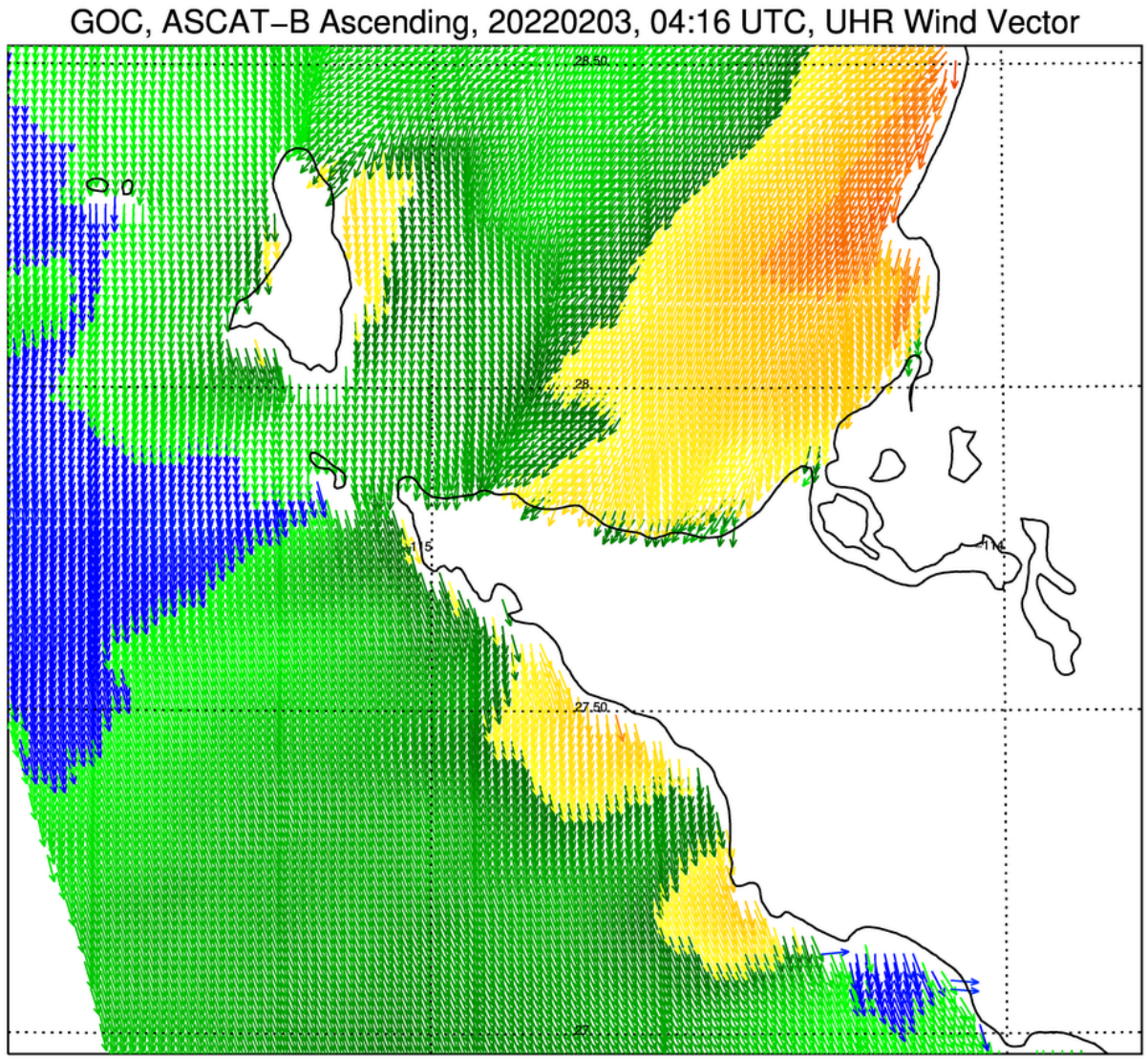
12.5km Winds



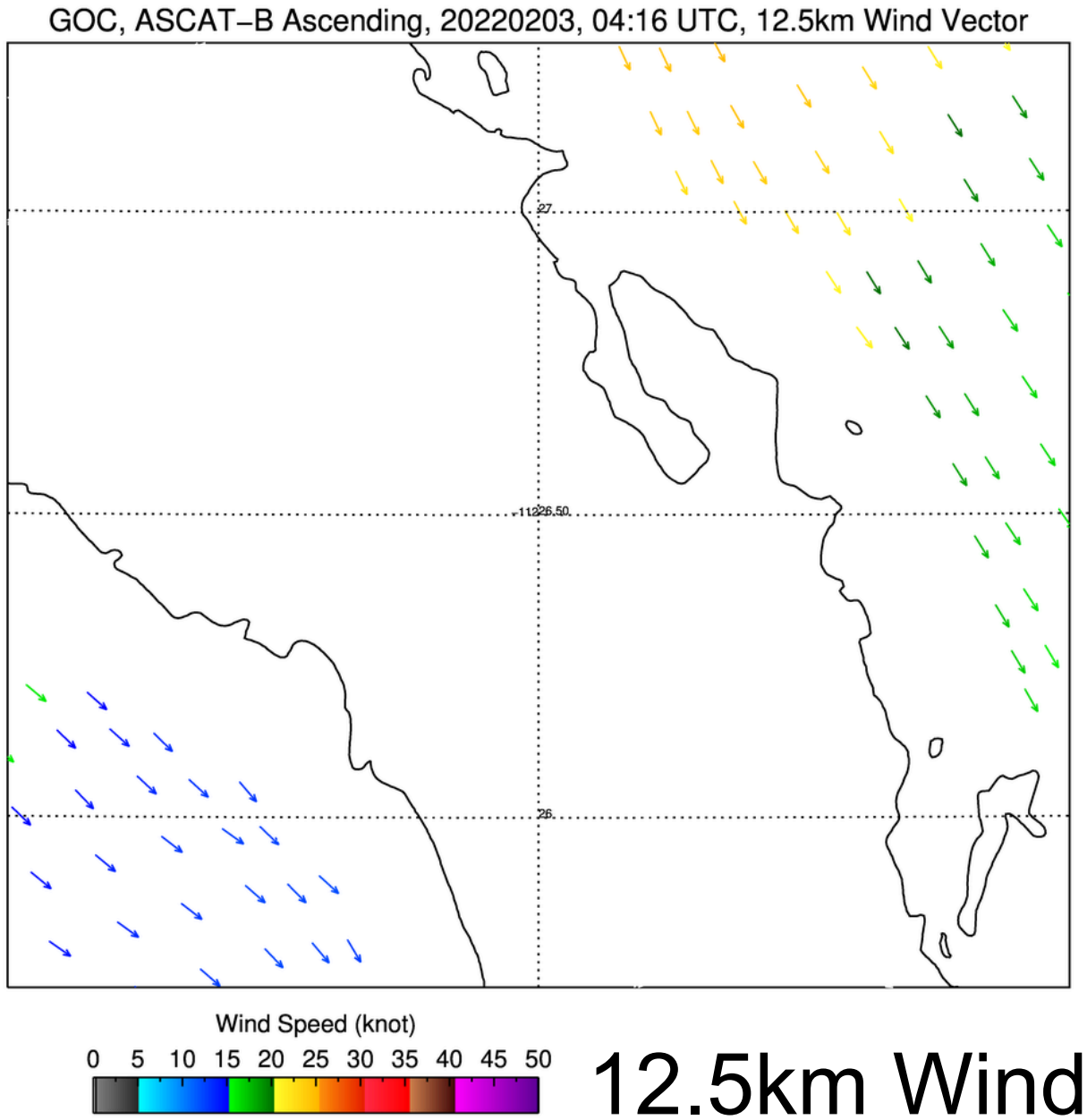
UHR Winds



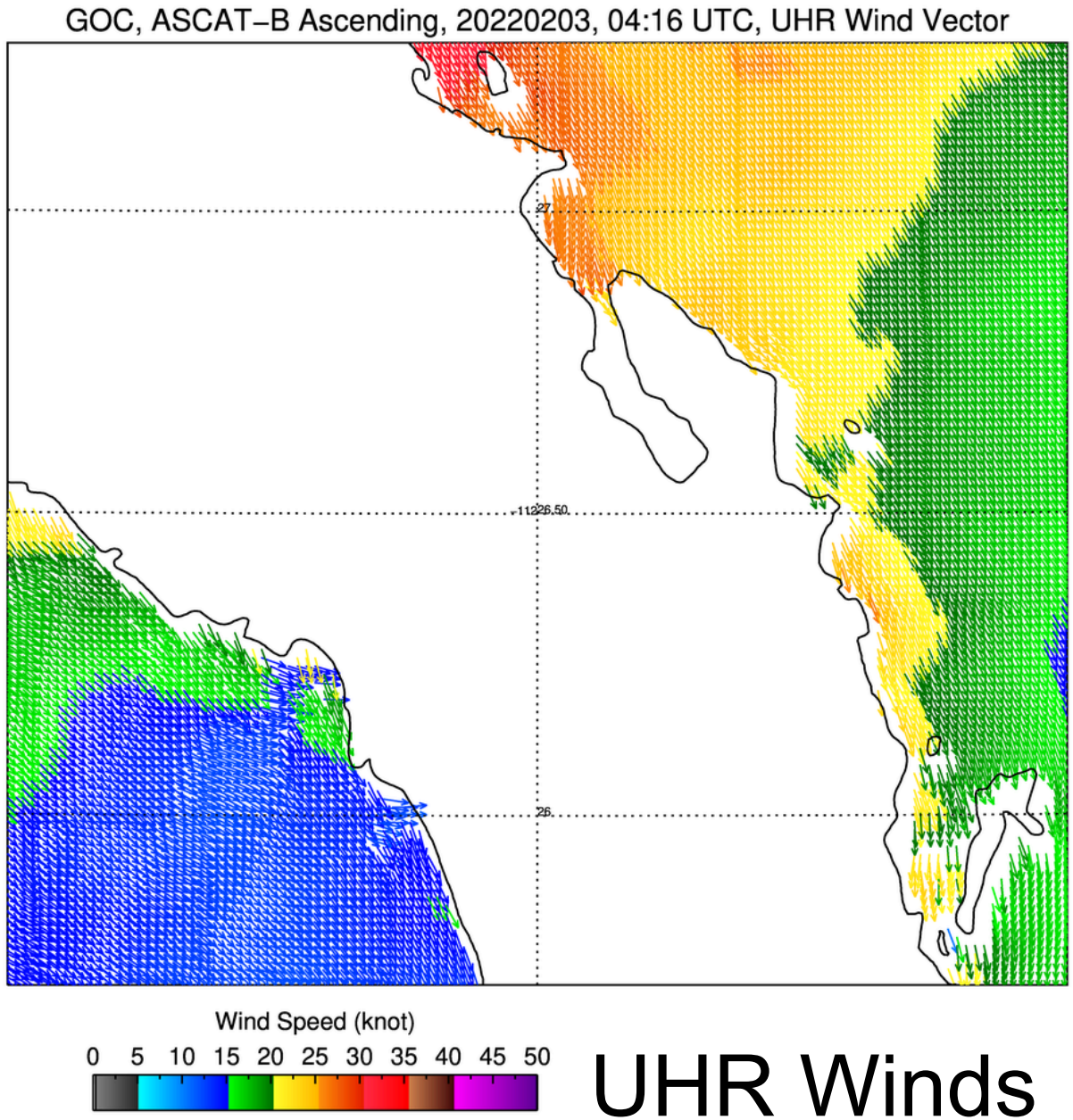
12.5km Winds



UHR Winds

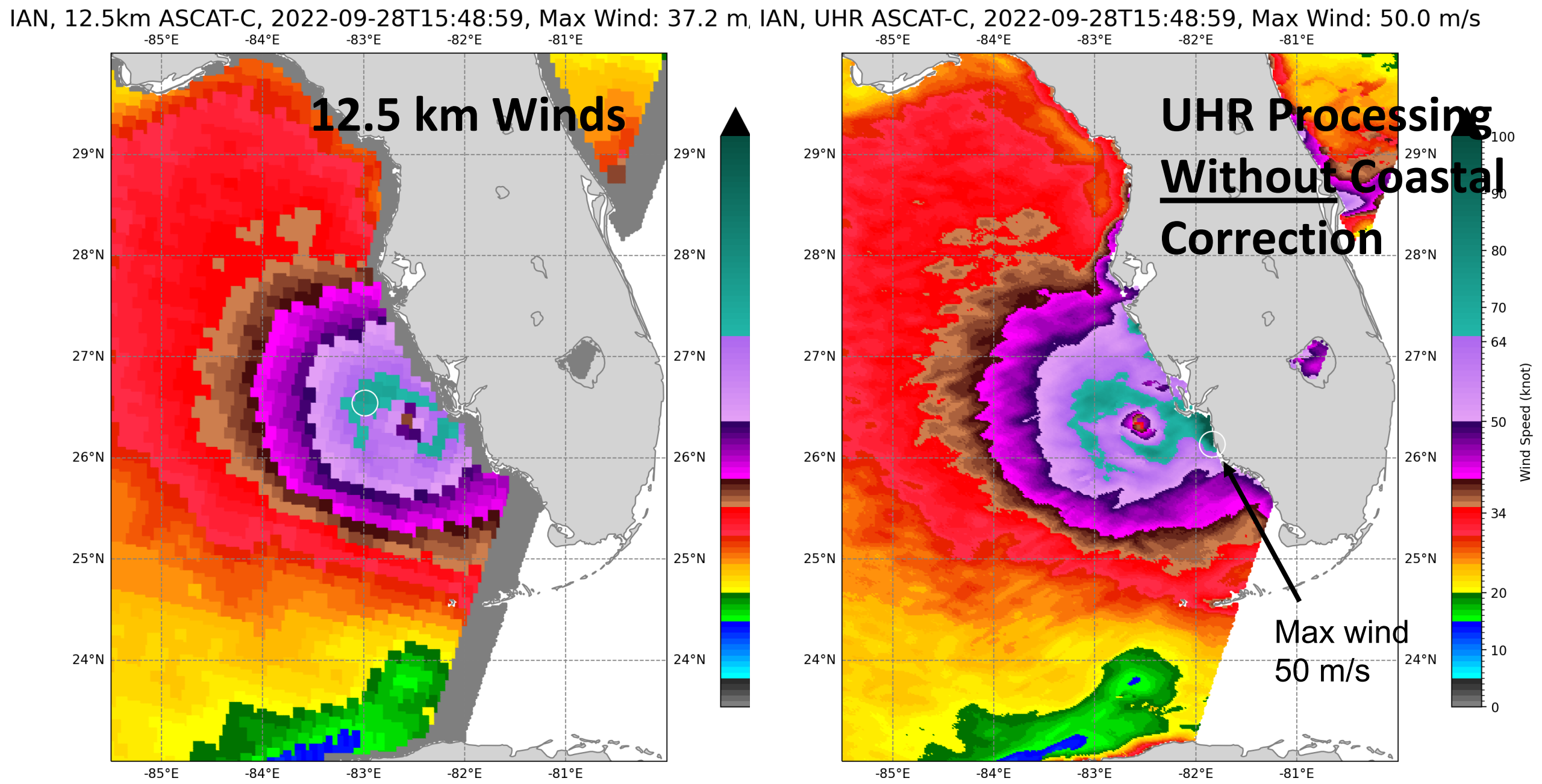


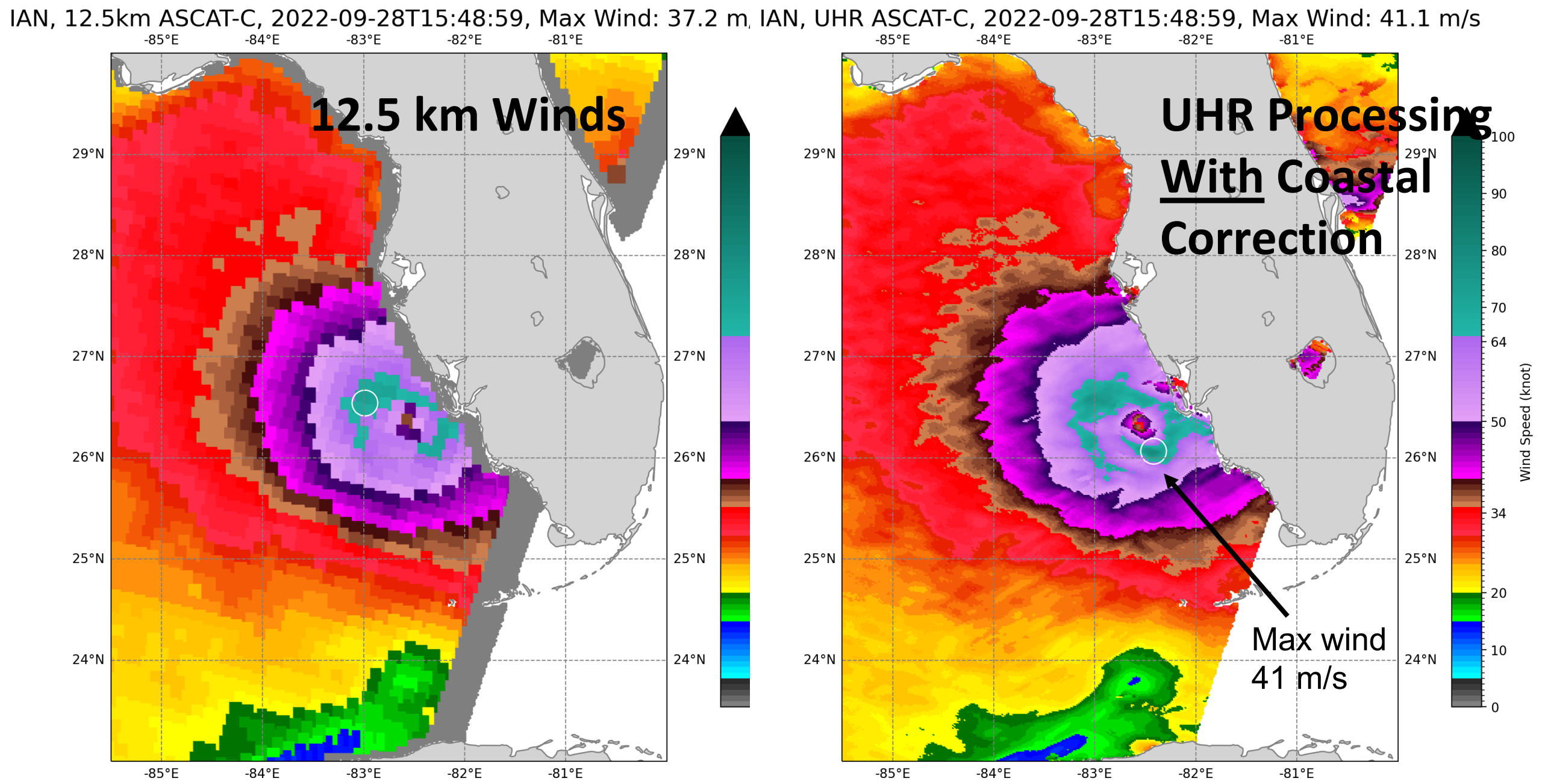
12.5km Winds



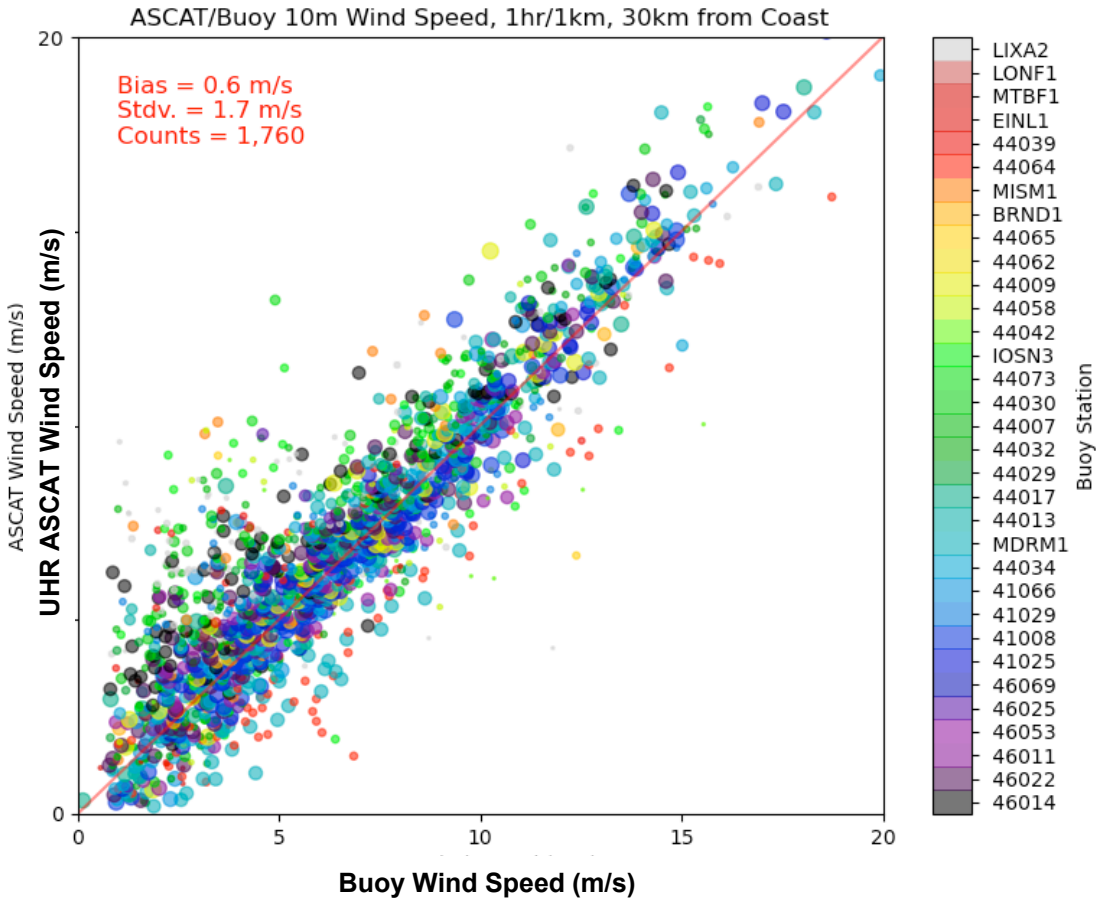
UHR Winds

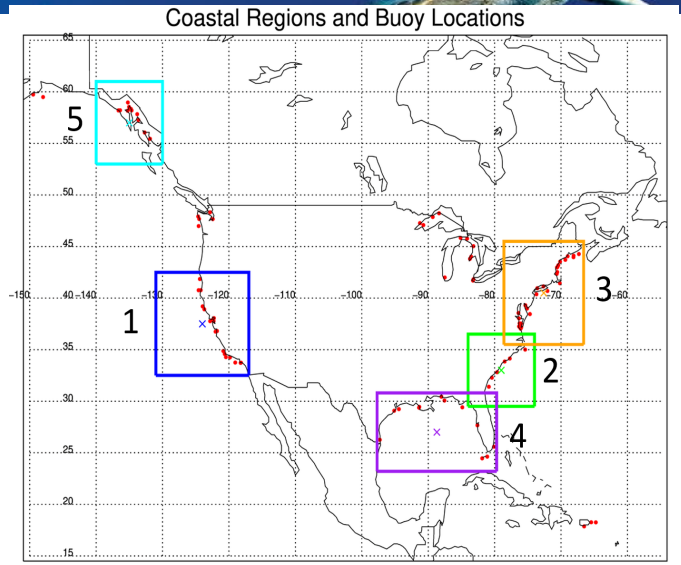
Case Study #2

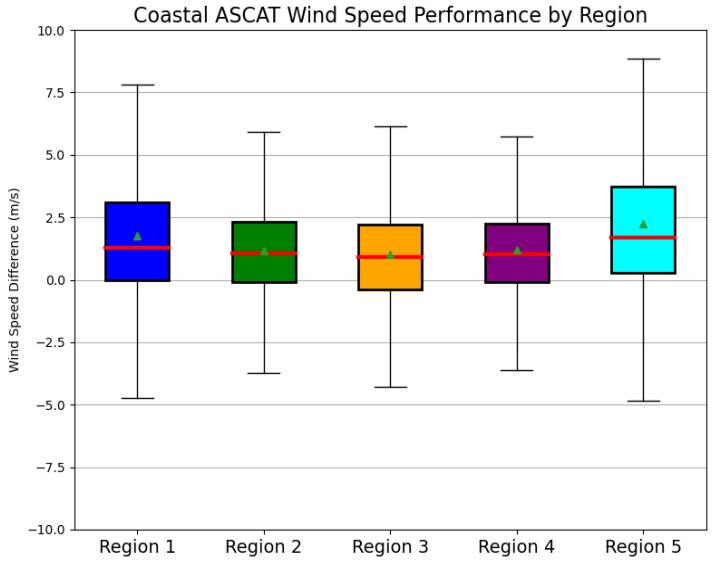

IAN, 12.5km ASCAT-C, 2022-09-28T15:48:59, Max Wind: 37.2 m
IAN, UHR ASCAT-C, 2022-09-28T15:48:59, Max Wind: 50.0 m/s
12.5 km Winds
UHR Processing Without Coastal Correction
Max wind 50 m/s
Wind Speed (knot)
-85°E
-84°E
-83°E
-82°E
-81°E
29°N
28°N
27°N
26°N
25°N
24°N
0
10
20
34
50
64
70
80
90
100


IAN, 12.5km ASCAT-C, 2022-09-28T15:48:59, Max Wind: 37.2 m
IAN, UHR ASCAT-C, 2022-09-28T15:48:59, Max Wind: 41.1 m/s
12.5 km Winds
UHR Processing
With Coastal
Correction
Max wind
41 m/s
Wind Speed (knot)
-85°E
-84°E
-83°E
-82°E
-81°E
29°N
28°N
27°N
26°N
25°N
24°N
0
10
20
34
50
64
70
80
90
100

UHR Coastal Wind Validation with Buoys

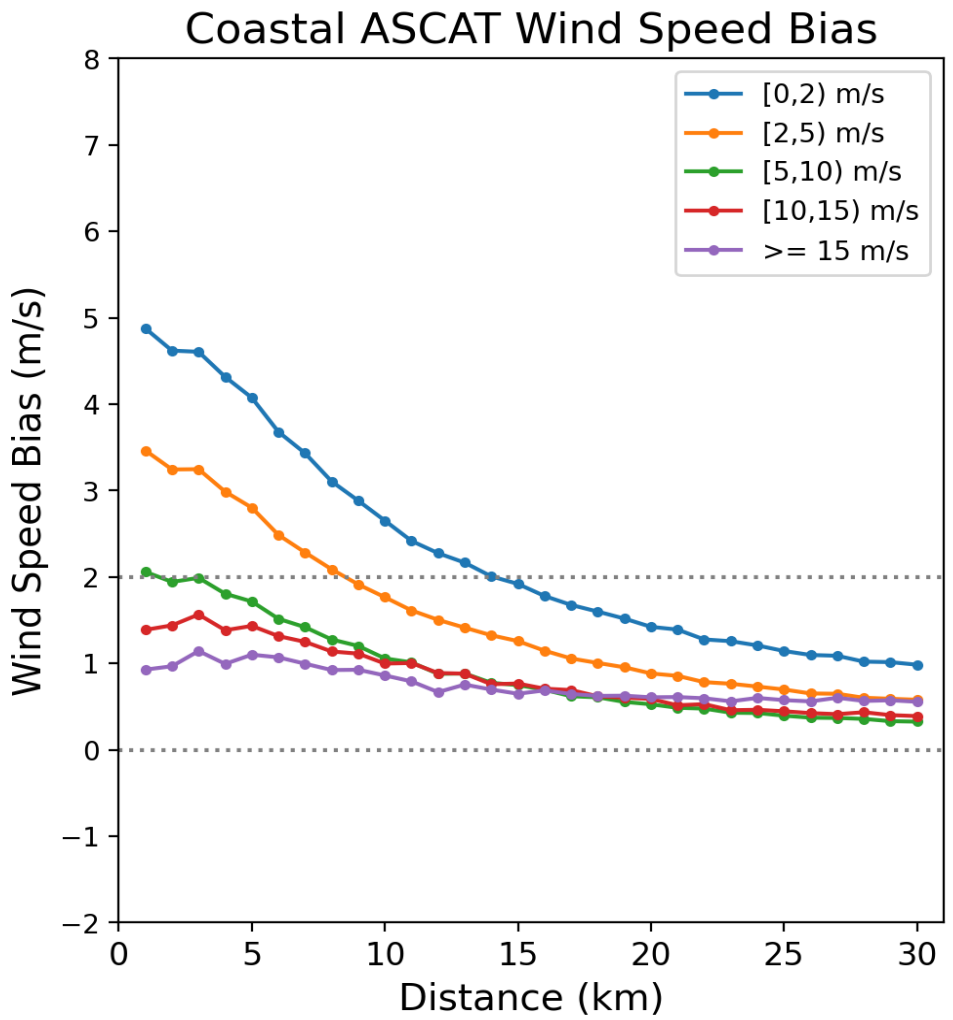


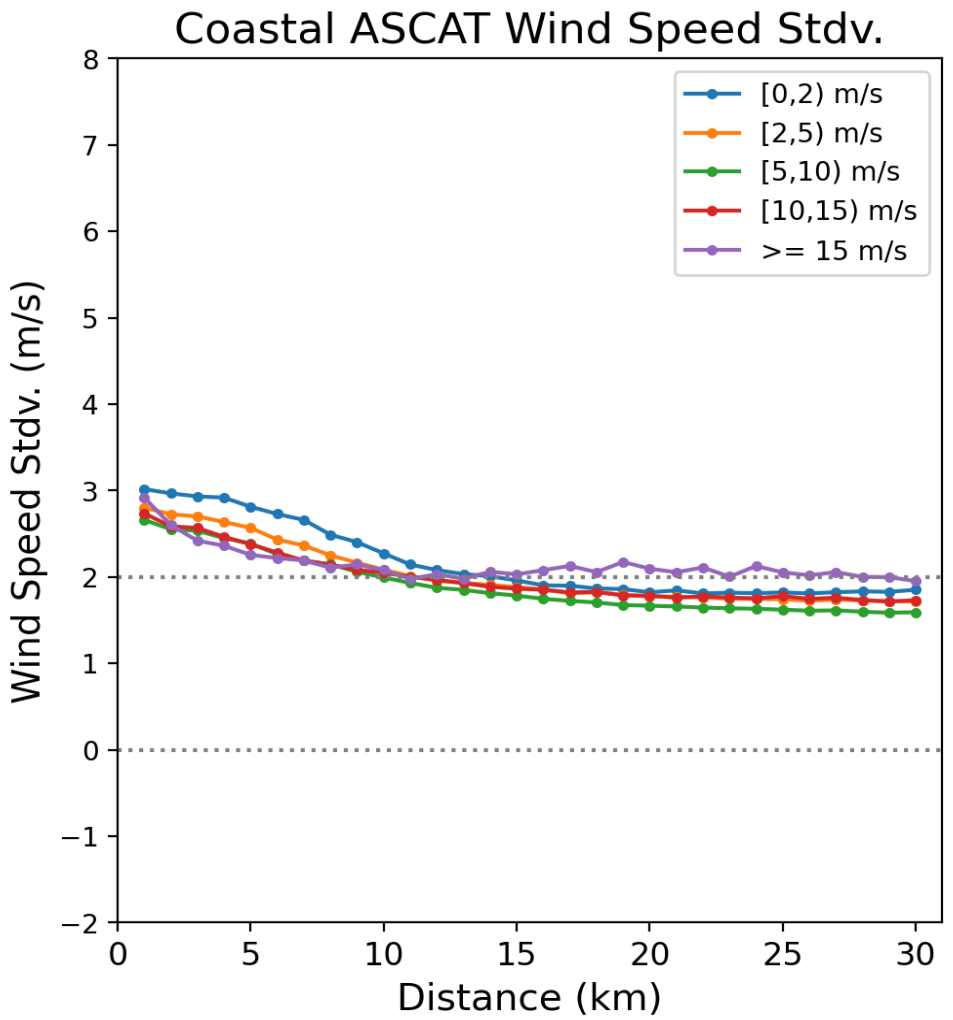




S. Soisuvarn, Z. Jelenak, P. S. Chang, Q. Zhu and C. G. Shoup, "High-Resolution Coastal Winds From the NOAA Near Real-Time ASCAT Processor," in IEEE Transactions on Geoscience and Remote Sensing, vol. 61, pp. 1-12, 2023, Art no. 5208612, doi: 10.1109/TGRS.2023.3279764.

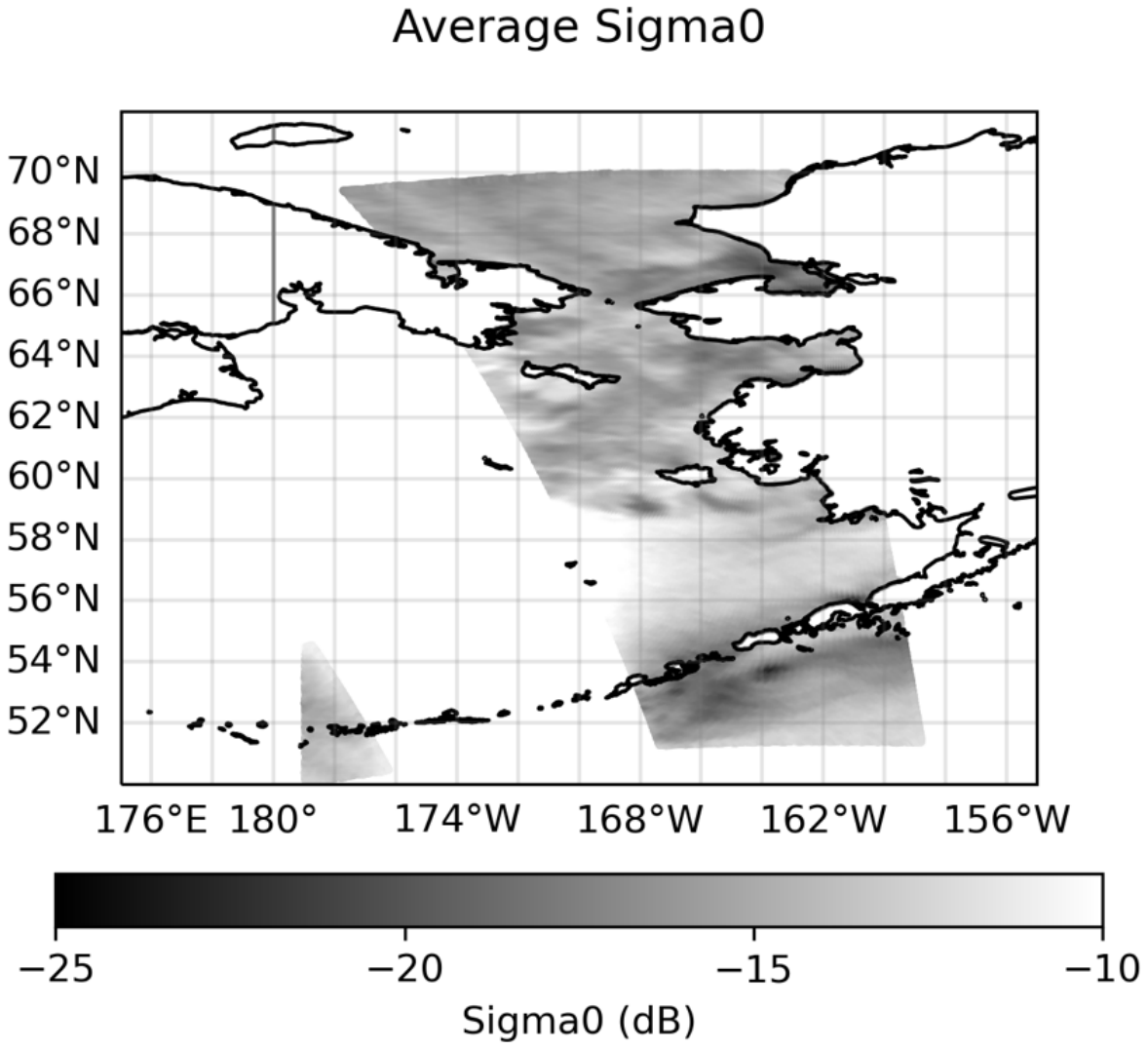
Coastal Winds Performance

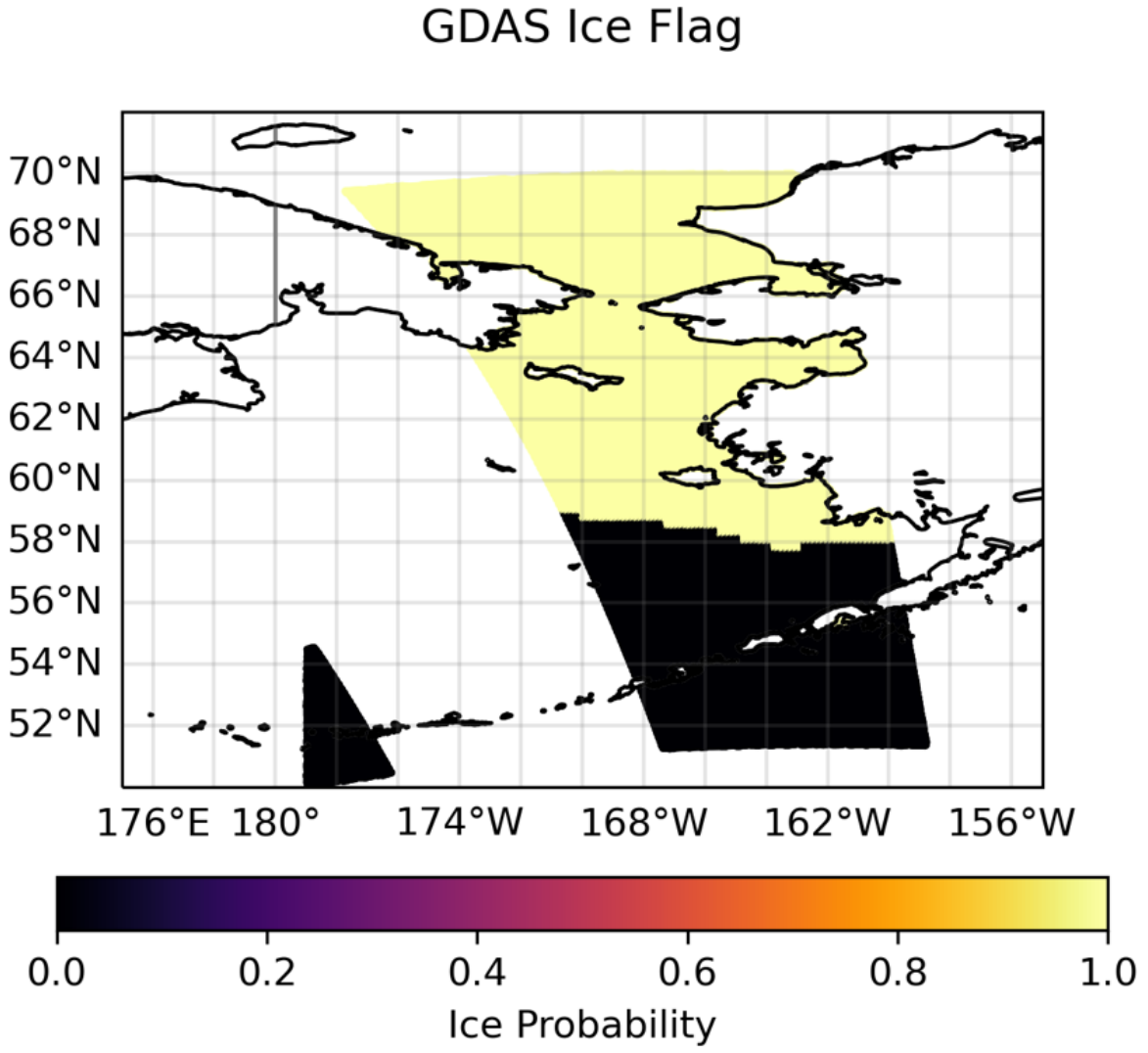




UHR ASCAT ice product

- In the high latitudes region where sea ice present, UHR ASCAT wind retrievals need to be flagged to avoid erroneous wind values.
- We introduce UHR sea ice flagging based on supervised machine learning (ML) approach.
  - Implement the Support Vector Machine (SVM) classification algorithm.
  - 6 UHR ASCAT variables are utilized to establish the correlation with the ice target using NWP ice flag.
    - Latitude, fore-aft, mid-fore, aft-mid sigma0's, wind speed and MLE.
- We used in-sample data extracted directly from the UHR observations instead of a large dataset. This allow a sufficiently small number of data point to train the ML model in NRT.
- UHR sigma0 and related variables can reveal features over ice.

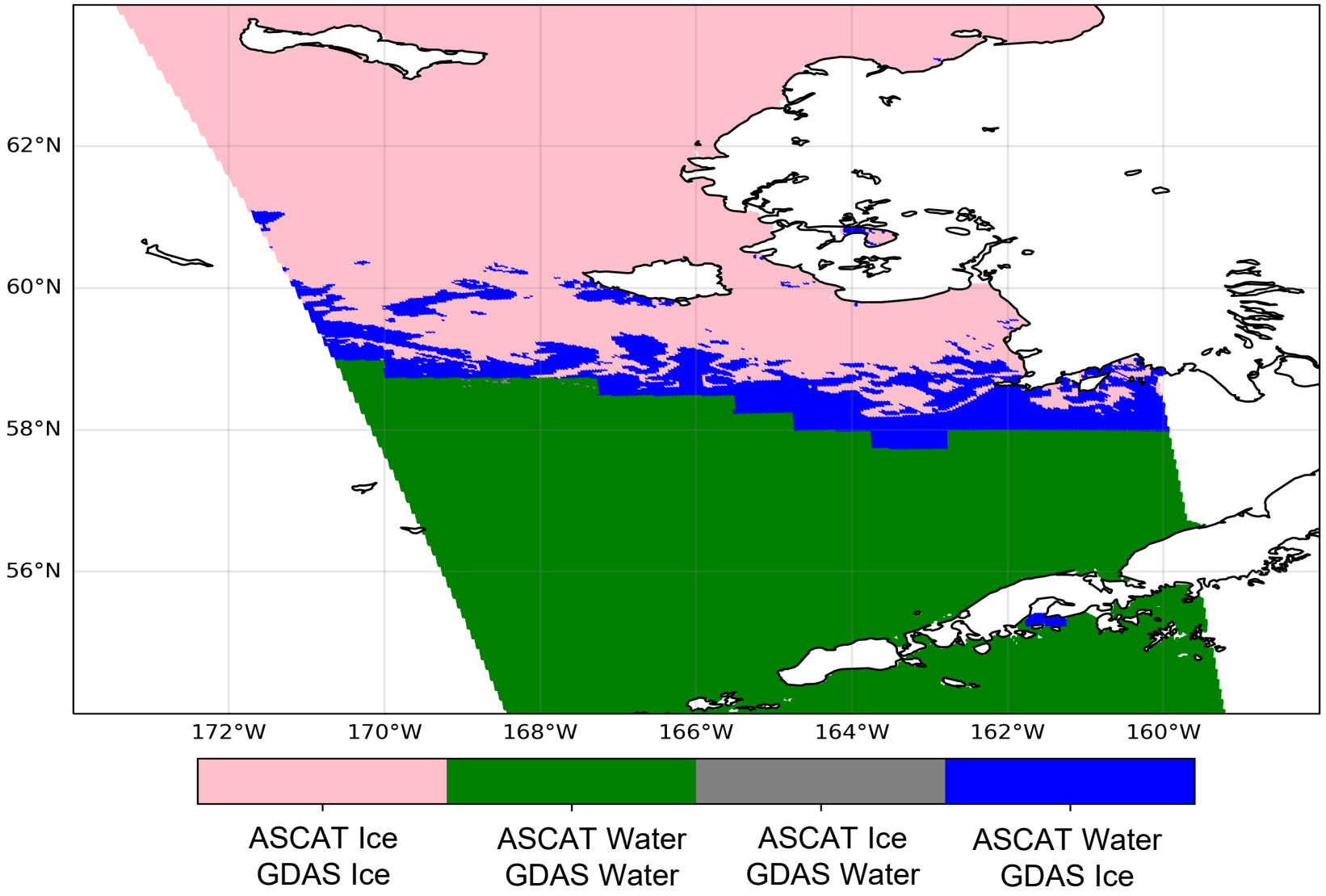




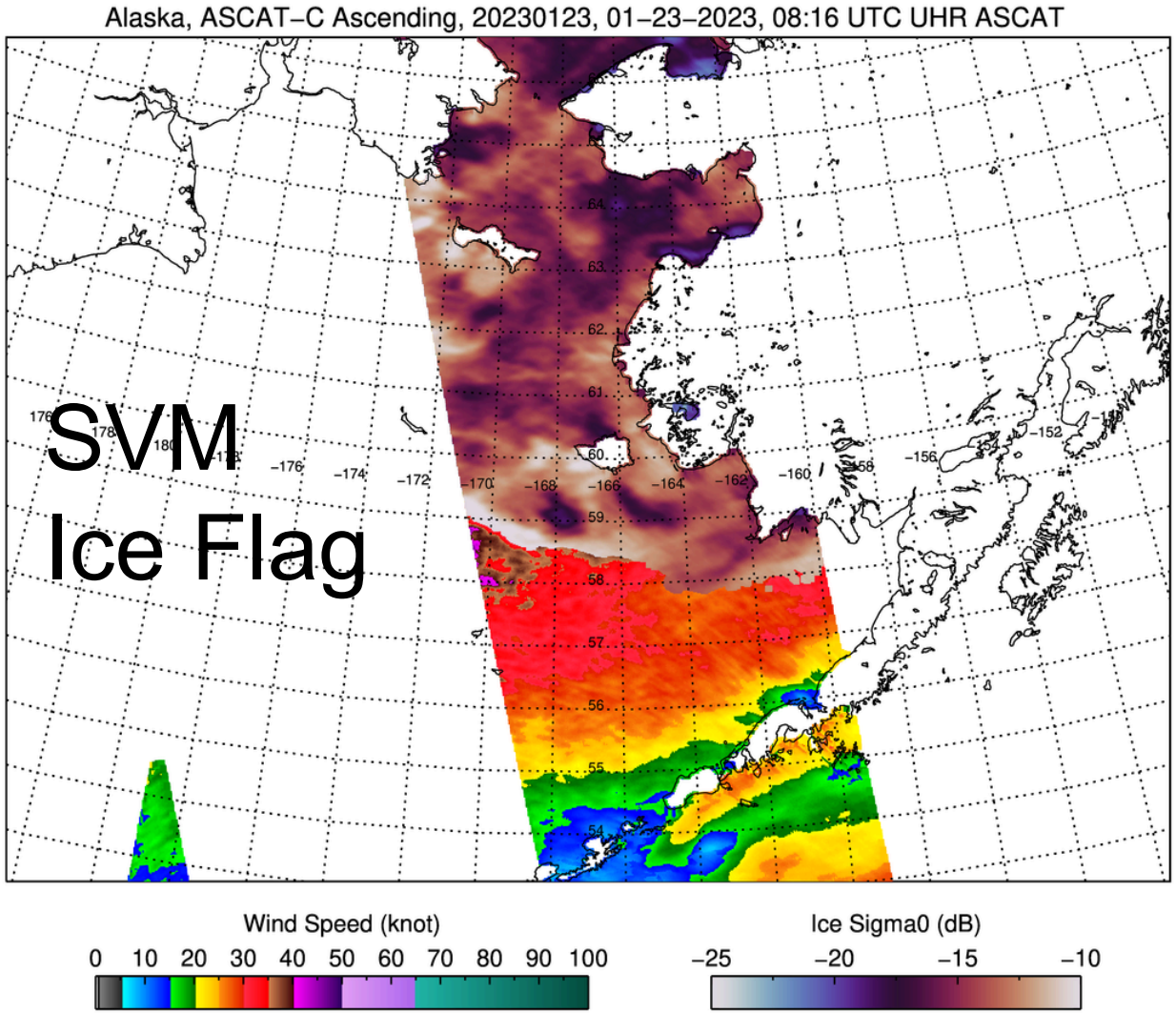
A UHR Sigma0 Training Feature

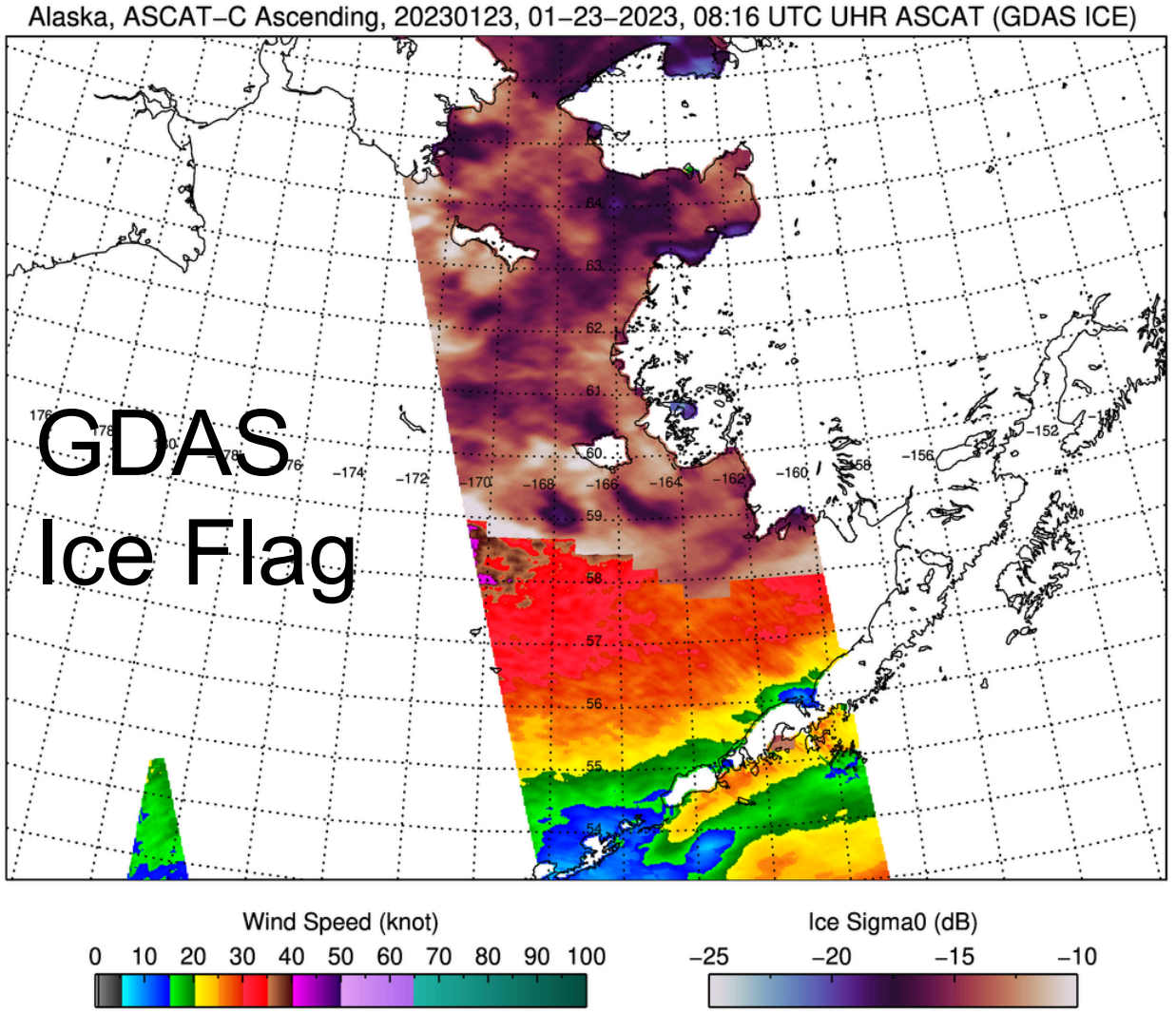
GDAS Sea Ice Target

UHR Sea Ice Confusion Matrix

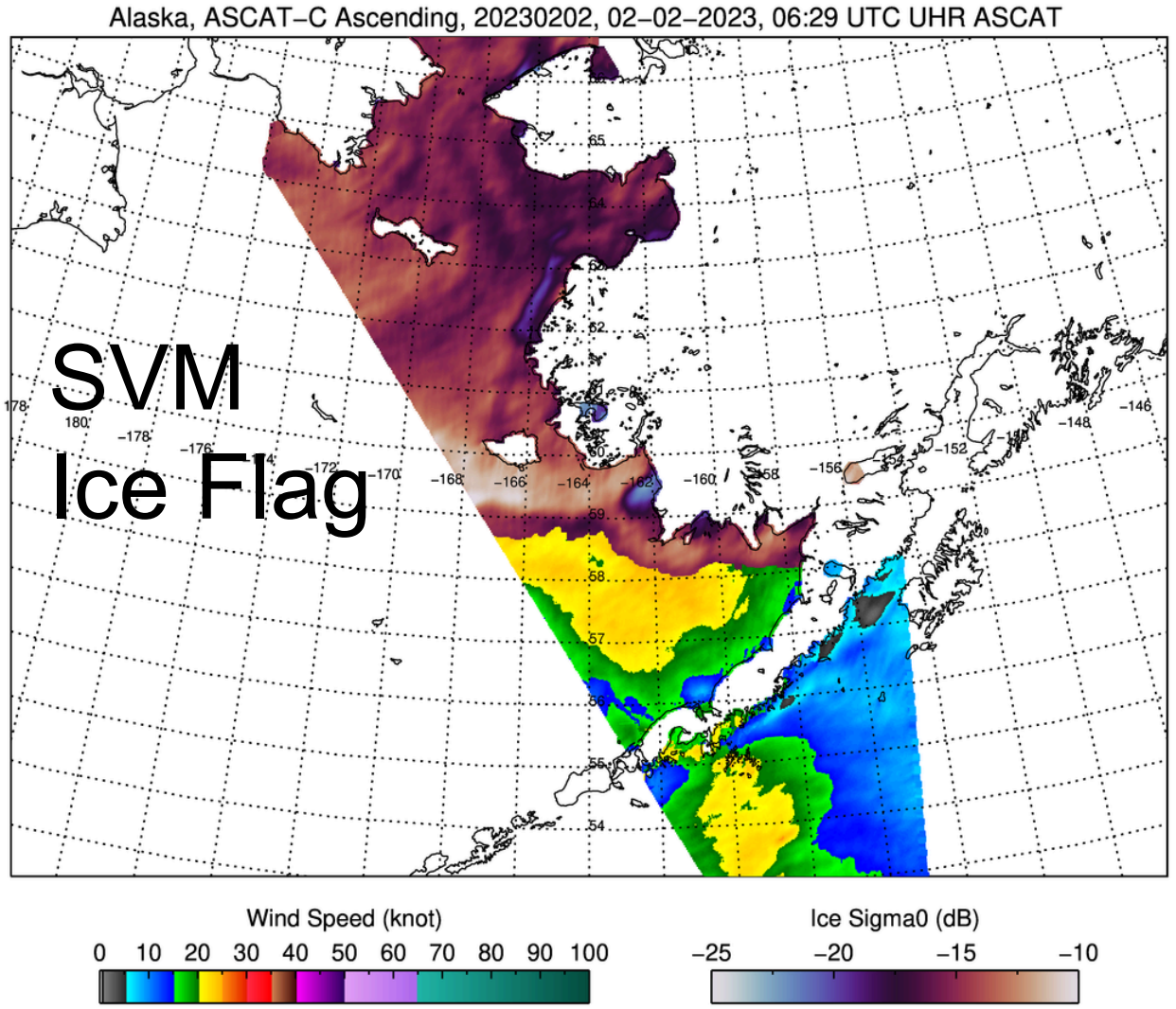


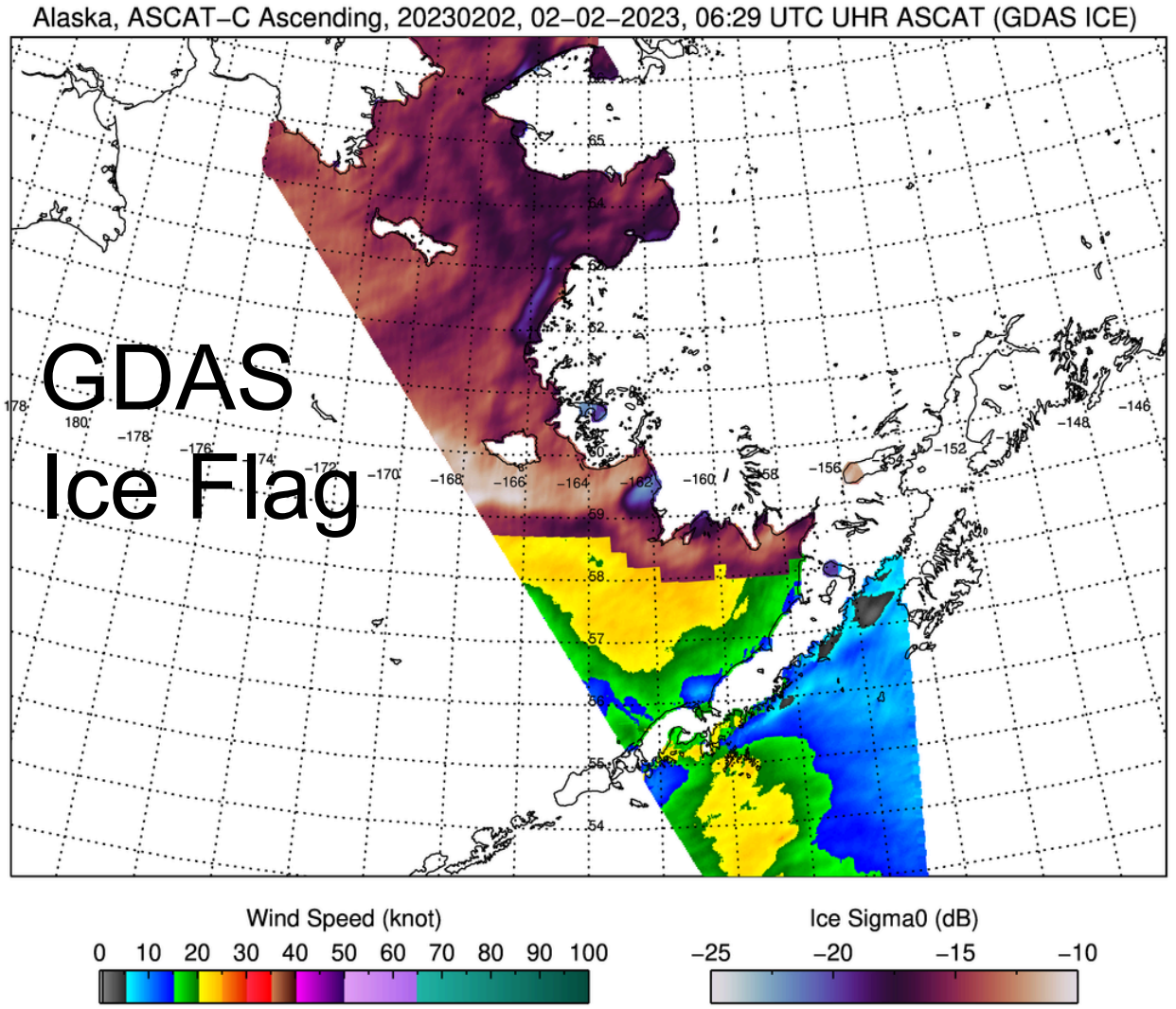
Case study on January 23, 2023





Case study on February 2, 2023



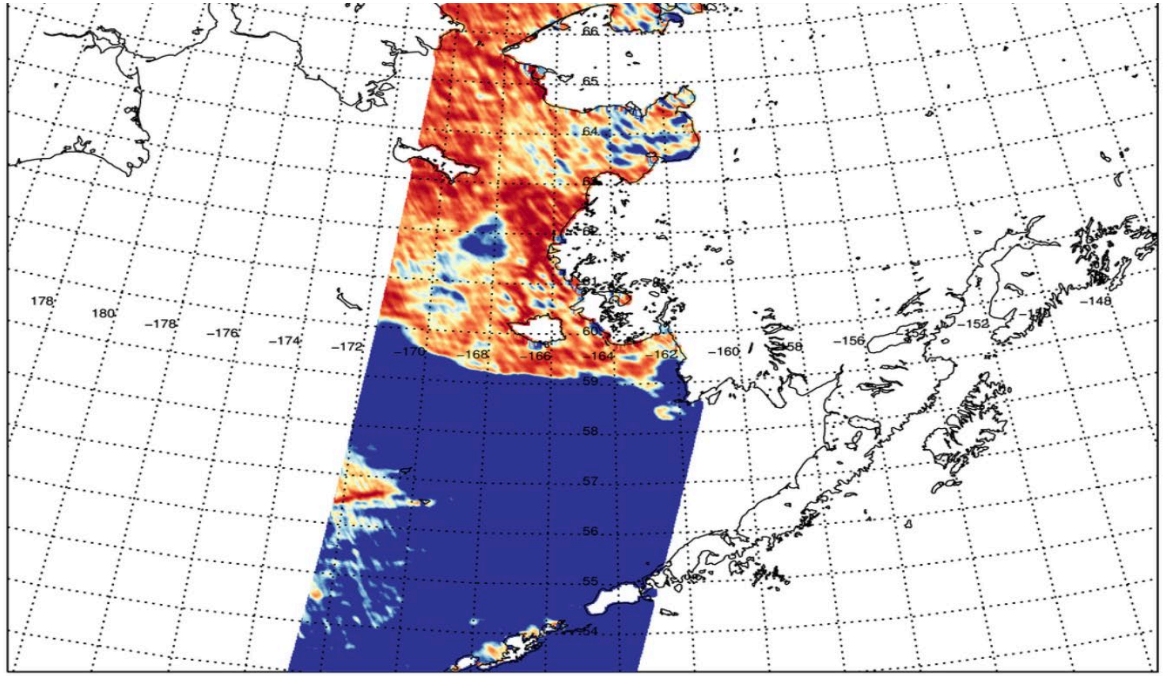


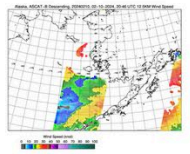
Variance of Sigma0 triple measurements within cell

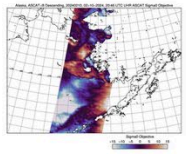
- Variance is usually very high over ocean and lower over ice
- Dependent on measurements geometry hence different variations between ascending/descending passes and left and right swaths
- Low variance over oceans is observed in very low wind cases and for certain wind directions
- Higher variance over ice indicate higher water content within cell

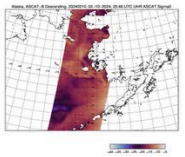
Product Description
- QuikSCAT/SeaWinds
- OSCAT
- ASCAT
- WindSAT
- Altimeter
- SMAP
- ERS-2
- SSM/I
- GCOMW1/AMSR2
- CYGNSS
- SCATSATS
- Aircraft Data
- Alaska ASCAT Coastal Products

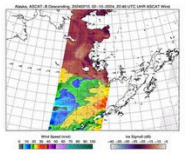
Data Products
- QuikSCAT/SeaWinds
- OSCAT
- RapidSCAT
- ASCAT (METOP-A)
- ASCAT (METOP-B)
- ASCAT (METOP-C)
- WindSAT
- Altimeter
- SMAP
- ERS-2
- SSM/I
- GCOMW1/AMSR2
- CYGNSS
- SCATSAT
- Aircraft Data
- Animated ASCAT Ice Products
- Alaska ASCAT Coastal Products

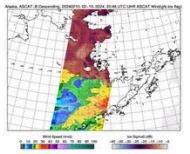



12.5KM Wind Speed


UHR Sigma0 Objective

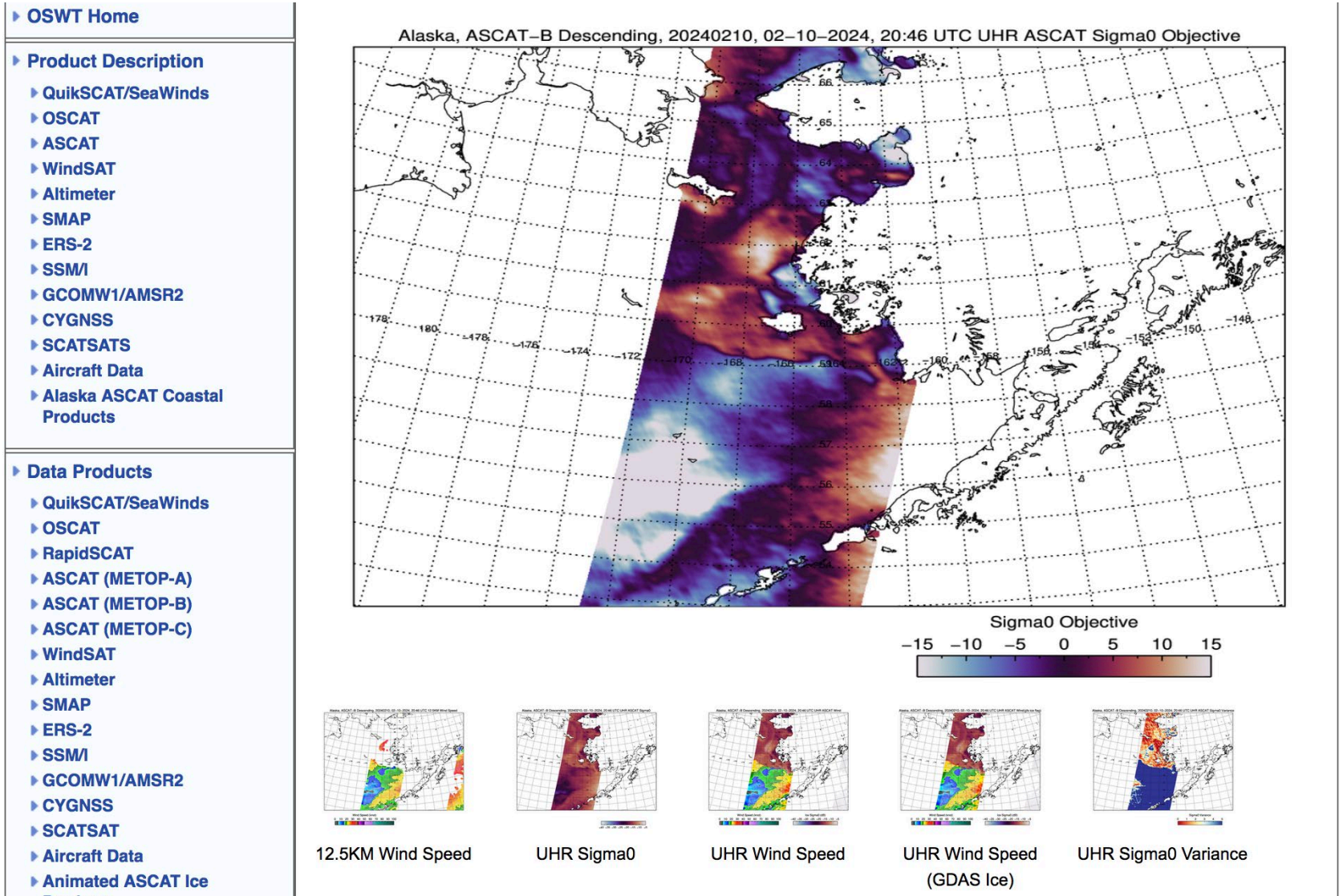

UHR Sigma0


UHR Wind Speed

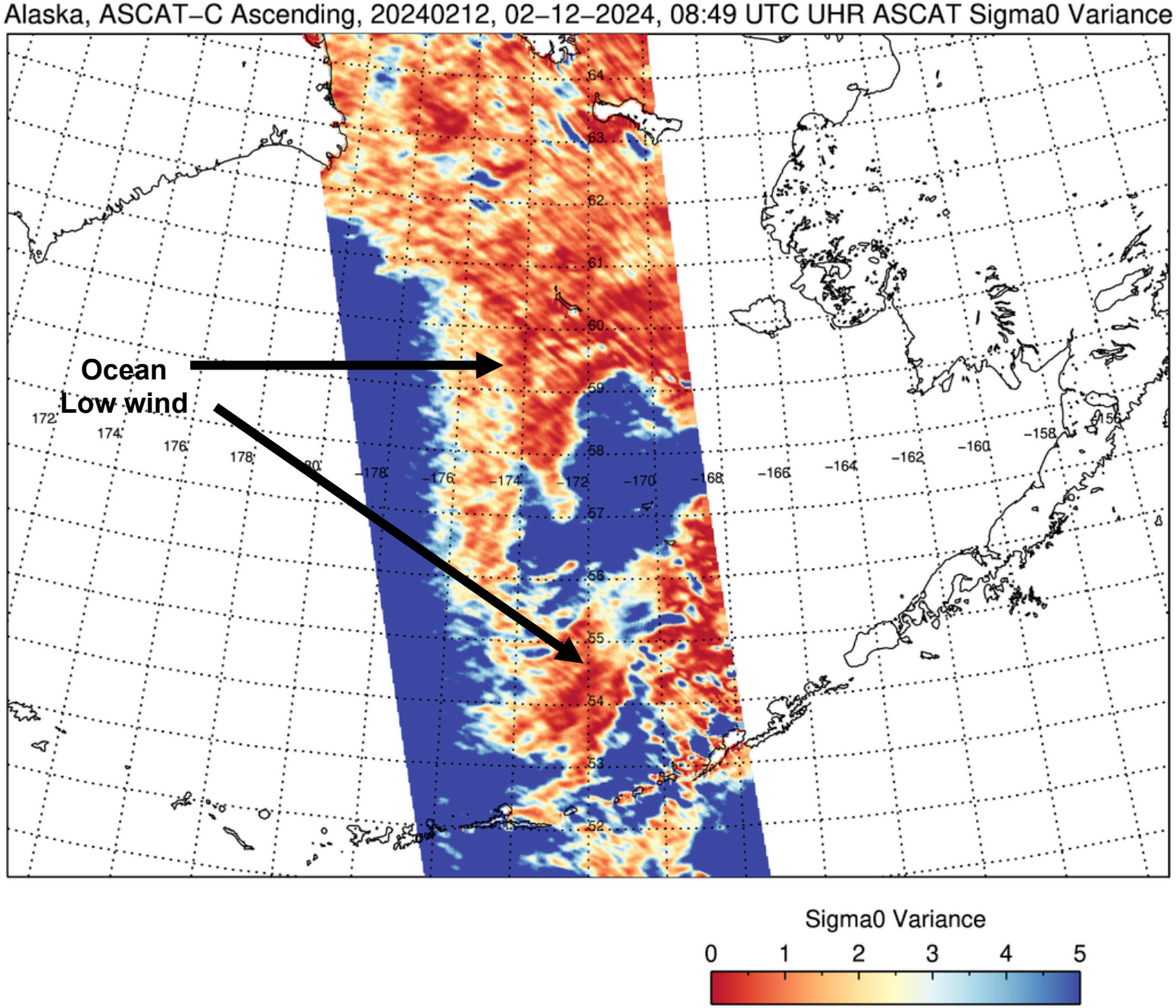

UHR Wind Speed (GDAS Ice)

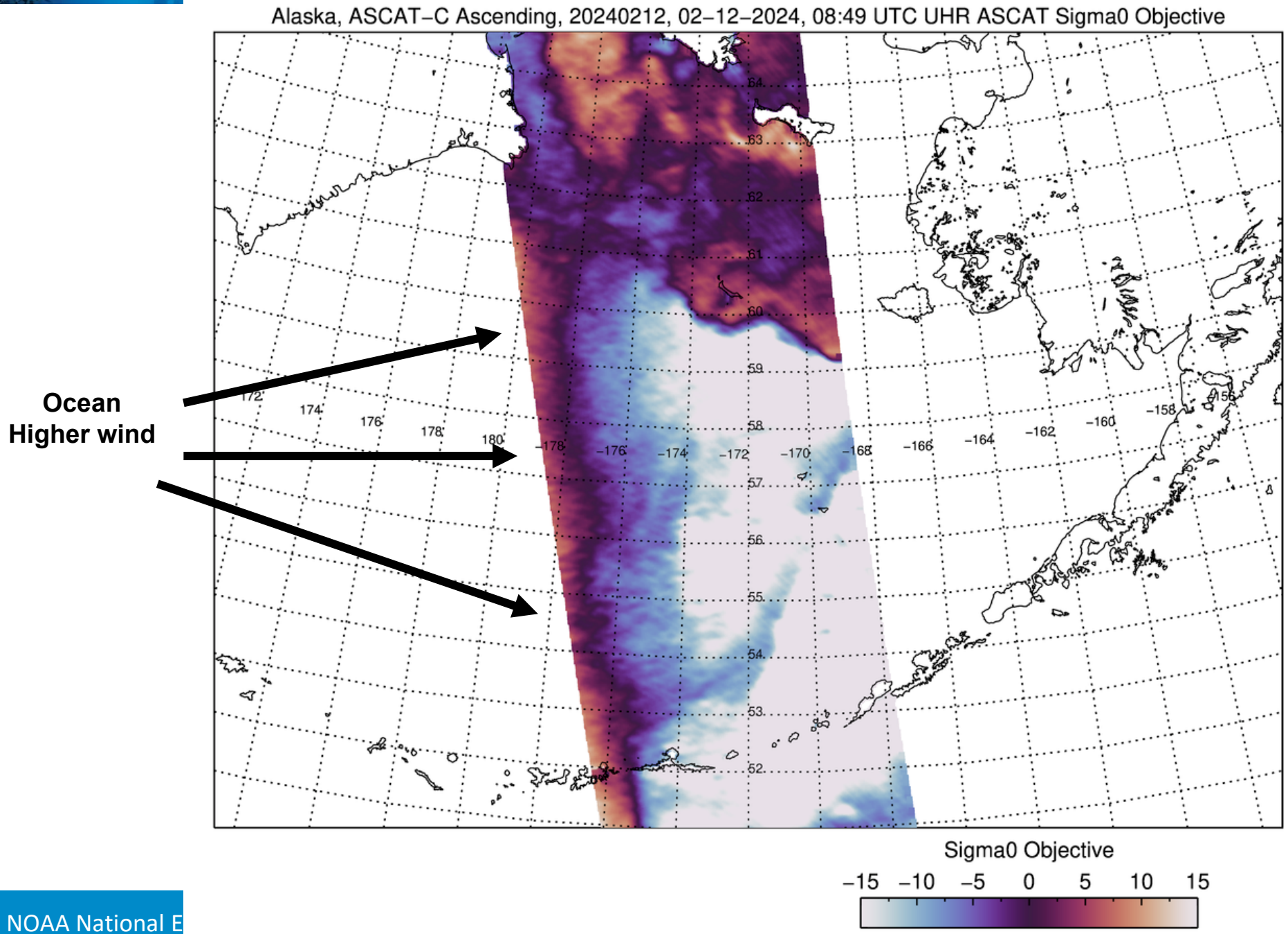
Sigma0 Objective = Ice Sigma0 – mean Ice Sigma0 model

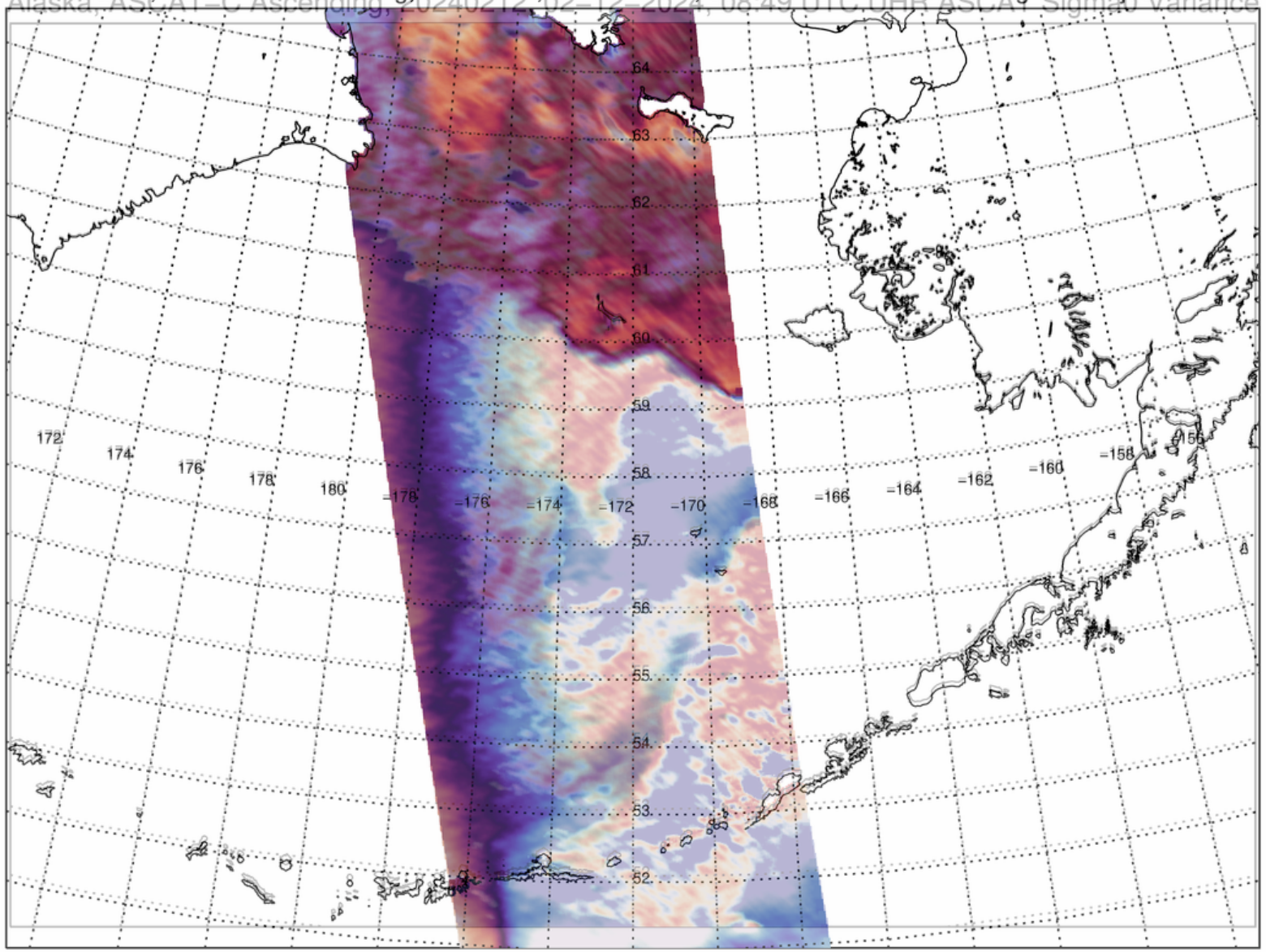
- Mean Ice Sigma0 model derived for all incidence and azimuth angle combinations
- Low value = thinner ice/ lower ice concentration
- High wind signal has similar response as ice



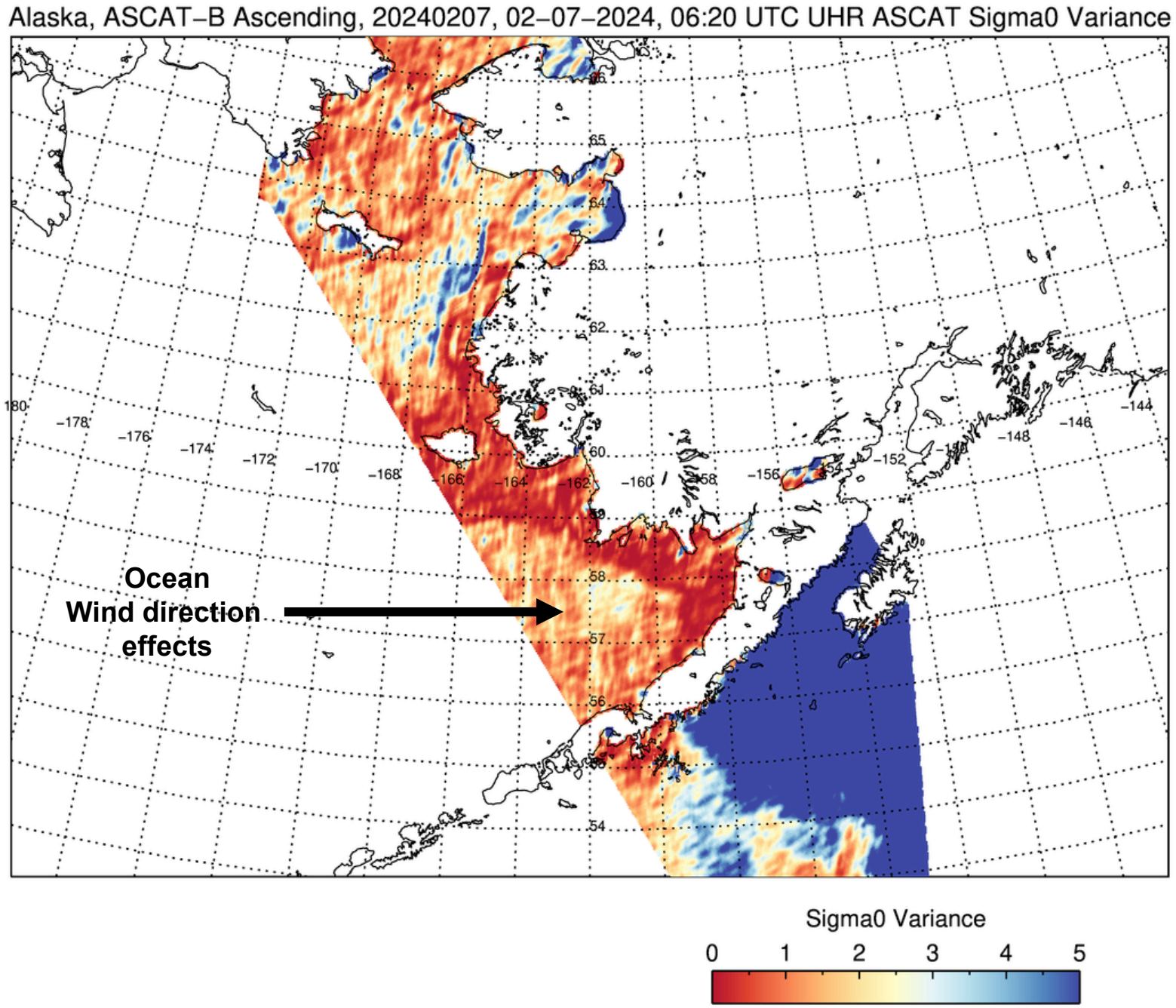
Case Study #1

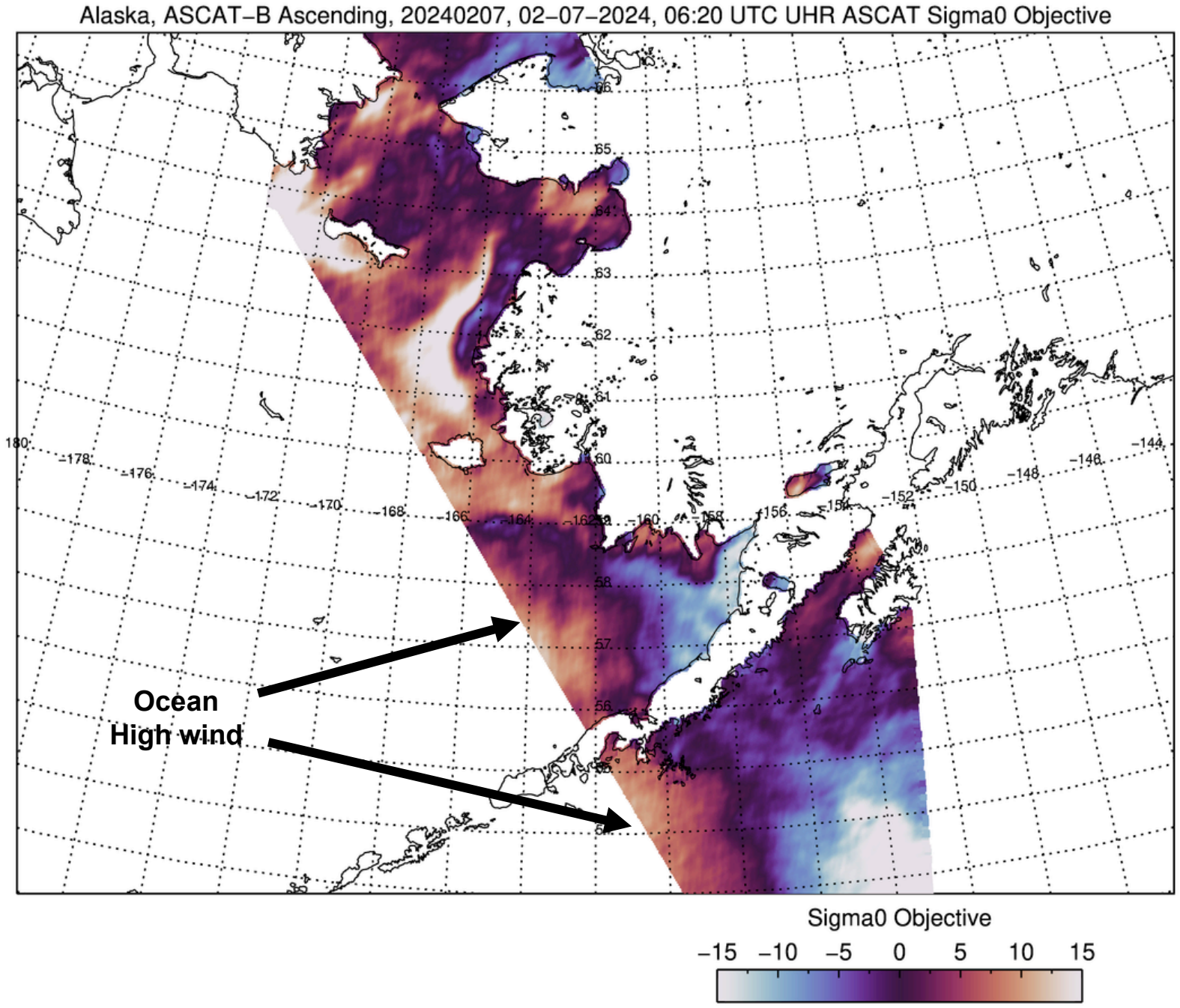

Alaska, ASCAT–C Ascending, 20240212, 02–12–2024, 08:49 UTC UHR ASCAT Sigma0 Variance
Ocean
Low wind
Sigma0 Variance
0 1 2 3 4 5

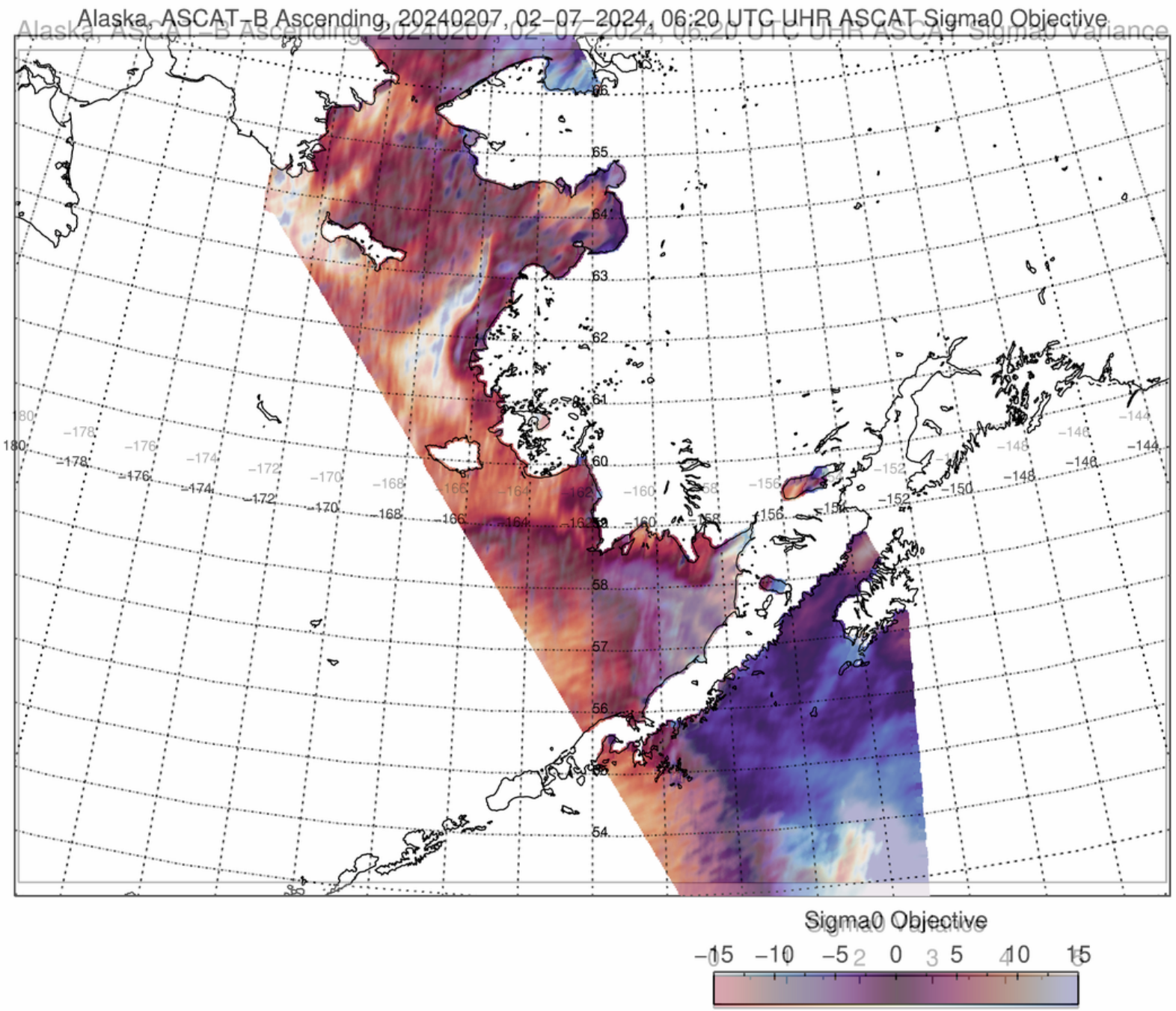

Alaska, ASCAT–C Ascending, 20240212, 02–12–2024, 08:49 UTC UHR ASCAT Sigma0 Objective
Ocean
Higher wind
Sigma0 Objective
−15 −10 −5 0 5 10 15


Alaska, ASCAT-C Ascending, 20240212, 02-12-2024, 08:49 UTC UHR ASCAT Sigma0 Objective
64
63
62
61
60
59
58
57
56
55
54
53
52
172
174
176
178
180
-178
-176
-174
-172
-170
-168
-166
-164
-162
-160
-158
-156
Sigma0 Objective
-15 -10 -5 0 5 10 15

Case Study #2


Alaska, ASCAT–B Ascending, 20240207, 02–07–2024, 06:20 UTC UHR ASCAT Sigma0 Variance
Ocean
Wind direction
effects
Sigma0 Variance
0 1 2 3 4 5


Alaska, ASCAT–B Ascending, 20240207, 02–07–2024, 06:20 UTC UHR ASCAT Sigma0 Objective
Ocean
High wind
Sigma0 Objective
−15 −10 −5 0 5 10 15


Alaska, ASCAT-B Ascending, 20240207, 02-07-2024, 06:20 UTC UHR ASCAT Sigma0 Objective
Sigma0 Objective
−15 −10 −5 0 5 10 15

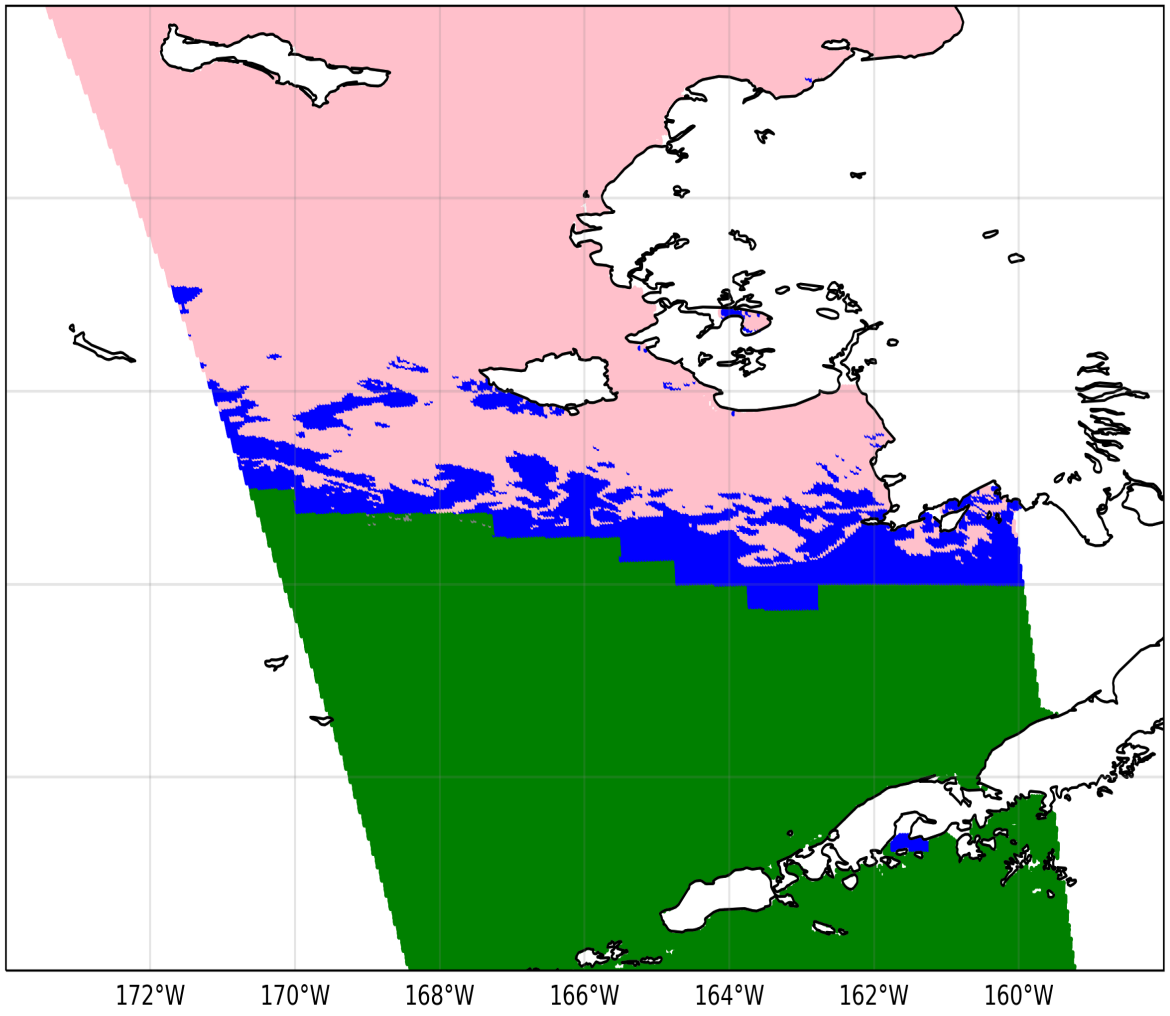
2024 Winter Flights

- 20240121
- 20240124 ice and ocean winds
- 20240128
- 20240130
- 20240201 ice and ocean winds
- 20240206 ice and ocean winds
- 20240208
- 20240209
- 20240212

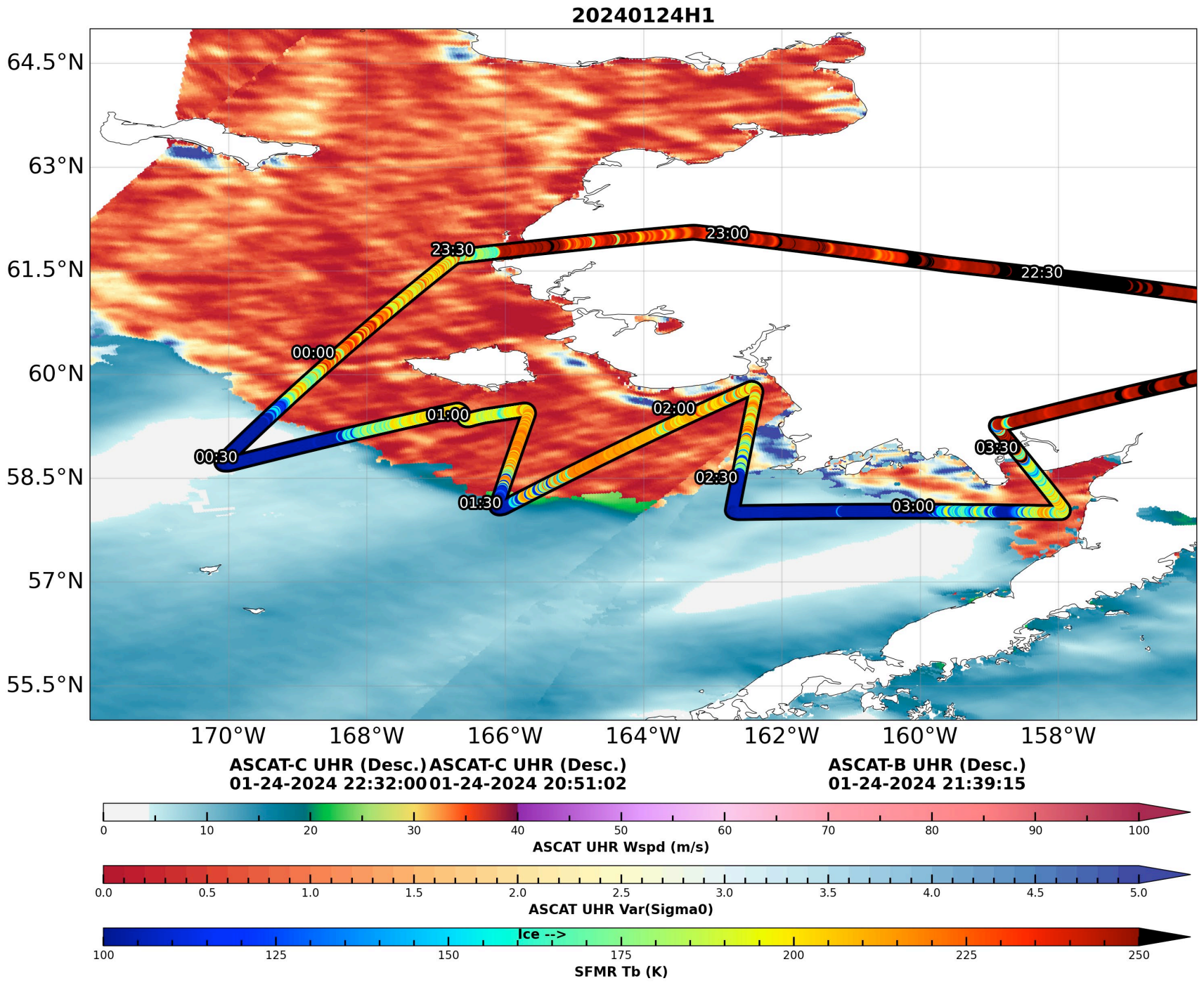


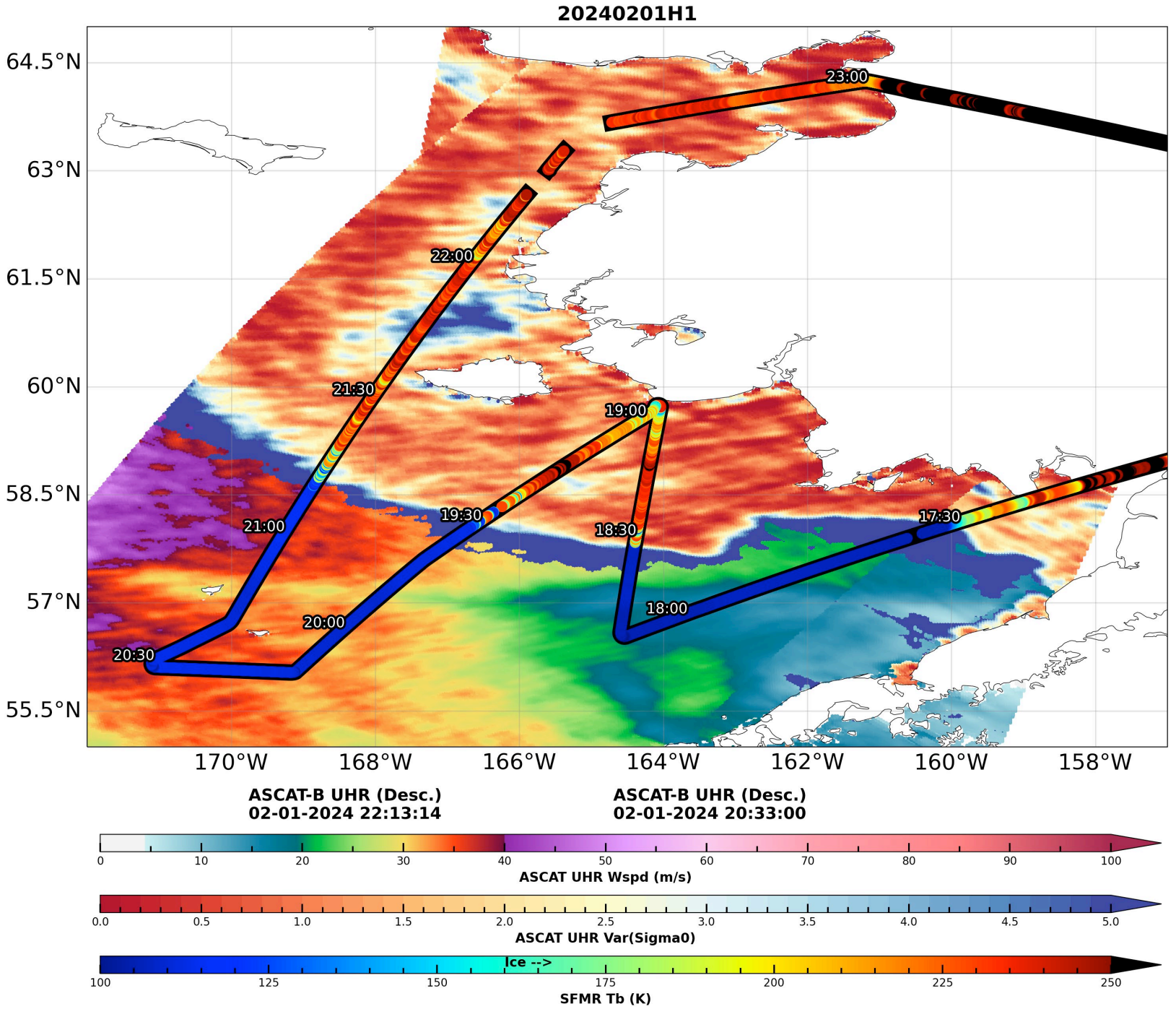


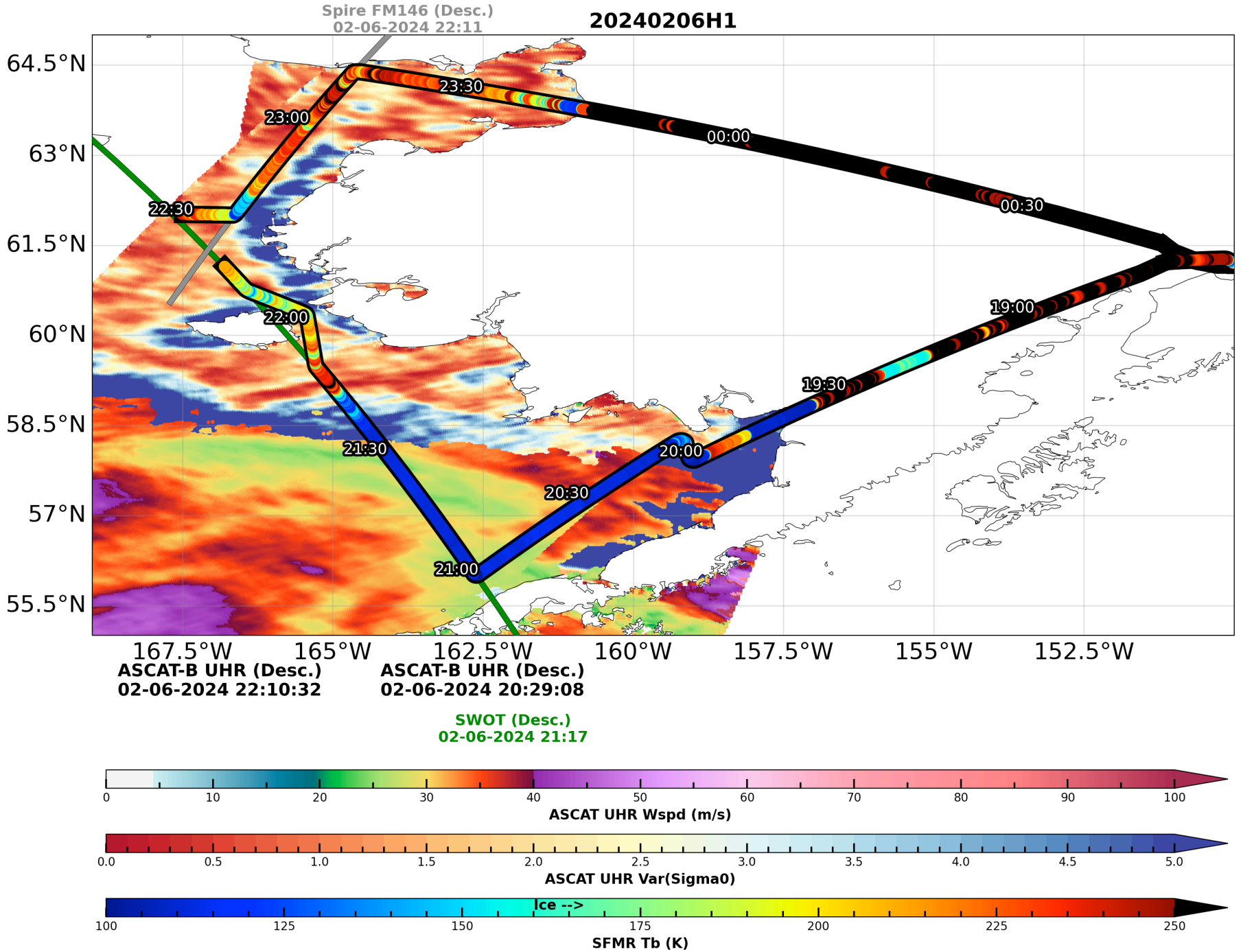
SVM Ice Prediction






20240124H1
64.5°N
63°N
61.5°N
60°N
58.5°N
57°N
55.5°N
170°W
168°W
166°W
164°W
162°W
160°W
158°W
23:30
23:00
22:30
00:00
01:00
02:00
00:30
01:30
02:30
03:30
03:00
ASCAT-C UHR (Desc.)
01-24-2024 22:32:00
ASCAT-C UHR (Desc.)
01-24-2024 20:51:02
ASCAT-B UHR (Desc.)
01-24-2024 21:39:15
0 10 20 30 40 50 60 70 80 90 100
ASCAT UHR Wspd (m/s)
0.0 0.5 1.0 1.5 2.0 2.5 3.0 3.5 4.0 4.5 5.0
ASCAT UHR Var(Sigma0)
Ice -->
100 125 150 175 200 225 250
SFMR Tb (K)


20240201H1
64.5°N
63°N
61.5°N
60°N
58.5°N
57°N
55.5°N
170°W
168°W
166°W
164°W
162°W
160°W
158°W
23:00
22:00
21:30
21:00
20:30
20:00
19:30
19:00
18:30
18:00
17:30
ASCAT-B UHR (Desc.)
02-01-2024 22:13:14
ASCAT-B UHR (Desc.)
02-01-2024 20:33:00
0
10
20
30
40
50
60
70
80
90
100
ASCAT UHR Wspd (m/s)
0.0
0.5
1.0
1.5
2.0
2.5
3.0
3.5
4.0
4.5
5.0
ASCAT UHR Var(Sigma0)
Ice -->
100
125
150
175
200
225
250
SFMR Tb (K)


Spire FM146 (Desc.)
02-06-2024 22:11
20240206H1
64.5°N
63°N
61.5°N
60°N
58.5°N
57°N
55.5°N
23:30
23:00
00:00
00:30
22:30
19:00
22:00
19:30
21:30
20:00
20:30
21:00
167.5°W
165°W
162.5°W
160°W
157.5°W
155°W
152.5°W
ASCAT-B UHR (Desc.)
02-06-2024 22:10:32
ASCAT-B UHR (Desc.)
02-06-2024 20:29:08
SWOT (Desc.)
02-06-2024 21:17
0
10
20
30
40
50
60
70
80
90
100
ASCAT UHR Wspd (m/s)
0.0
0.5
1.0
1.5
2.0
2.5
3.0
3.5
4.0
4.5
5.0
ASCAT UHR Var(Sigma0)
Ice -->
100
125
150
175
200
225
250
SFMR Tb (K)

Summary

- UHR ASCAT wind processing reveals finer spatial details.
- UHR land contamination removal is required for accurate wind retrievals in coastal regions.
- UHR ASCAT ice processing reveals a more detailed ice edge and ice features.
- UHR ASCAT coastal wind and ice products are processed in near real-time, and the data is available for download.

https://manati.star.nesdis.noaa.gov/datasets/AscatCoastalUHR.php

https://manati.star.nesdis.noaa.gov/datasets/AlaskaASCATCoastal.php

Backup slides

Coastal Winds from NOAA Near Real-Time SCATSAT-1 Scatterometer Processor

Seubson Soisuvarn[1, 2], Zorana Jelenak[1, 2], Paul Chang[1] and Qi Zhu[1, 3]
[1]*NOAA/NESDIS/Center for Satellite Applications and Research,* [2]*UCAR,* [3]*Global Science & Technology Inc.*
College Park, MD, USA
seubson.soisuvarn@noaa.gov

***Abstract*—The NOAA Operational SCATSAT-1 scatterometer ocean surface wind products are produced at a 12.5-25 km resolution. While they provide invaluable data over the open ocean, the wind retrievals stop short of providing any useful wind data near the coast. In order to retrieve winds in coastal zones, an enhanced resolution and land contamination removal algorithm has been developed. We show that the land contamination removal alone is not enough to get the wind retrievals closer than 15-25 km from the coast. In this paper, we develop a land contamination correction approach to get the winds closer to the coast. Together with a post wind retrieval processing we manage to retrieve winds up to 2.5 km from the coast. The coastal wind speeds are validated against NWP model winds for the U.S. Northeastern coastal zone. The performance shows a mean bias of -0.2 m/s and standard deviation of 2.9 m/s, which are comparable to the performance of the enhanced resolution open ocean wind product from the SCATSAT-1.**

Keywords—Scatterometer, Coastal Winds, Resolution Enhancement.

I. Introduction

The SCATSAT-1 scatterometer, launched by Indian Space and Research Agency (ISRO) on September 26, 2016, is an active microwave sensor that provided ocean surface wind vectors over the global oceans to world's operational weather and research communities until it stopped its operations in March 2021. The SCATSAT-1 measures the normalized radar cross section (NRCS) or sigma0 using a pencil-beam antenna from the wind roughened ocean surface by measuring the return radar pulses transmitted at a Ku-band frequency. The wind inversion algorithm is then used to derive wind vectors from a combination of sigma0 measurements at different polarization, azimuth and incidence angles. NOAA acquired and processed SCATSAT-1 wind data in near real-time since 2017 [1]. NOAA wind products were provided at 12.5 and 25 km spacing. While the SCATSAT-1 provides invaluable data over the open ocean, the retrievals stopped short of providing any wind estimates closer than15-20 km of the coasts due to land contamination of suited to provide this information within coastal zones, their availability is limited.

In order to retrieve winds closer to the coast, an enhanced resolution processing technique and the land contamination removal algorithm for pencil beam scatterometers was developed [2], which we tested on the SCATSAT-1 sigma0 measurements. While winds can be retrieved up to 20 km, with this method, most inner coastal areas are still devoid of data. In order to close this gap, following the approach developed by [2-4], we extended the algorithm to obtain wind retrievals as close as 2.5 km off the coast.

In this paper, we first discuss the baseline enhanced resolution coastal sigma0 processor and land contamination rejection criteria. In section II a thorough analysis of land contamination signal is presented. In section III, using the land contamination signal and land contamination ratio, we show that the measured sigma0 can be corrected even within the most inner coastal region. The initial wind retrievals resulting from land corrected sigma0's, post wind retrievals processing and final wind retrievals are presented and validated in section IV. The validation results are encouraging and show that the coastal winds from SCATSAT-1 within a few kilometers are indeed feasible. Final conclusions are stated in section V.

II. Land Contamination Signal

A. Enhanced Resolution Processing

The SCATSAT-1 enhanced resolution can be achieved by taking advantage of the overlapping regions of the radar echo that are separated by the Doppler frequency shift known as "slices" as presented in [5]. For the horizontal and vertical beams there are up to 9 or 15 slices available, respectively. The SCATSAT-1 antenna gain pattern projection on the surface, also known as the exact spatial response function (SRF) of each slice, is presently unknown, therefore, an estimated SRF was used instead. A half-sinewave gain pattern is assumed for each slice. A rectangular shape contour with a dimension of ~ 6 km in the

S. Soisuvarn, Z. Jelenak, P. Chang and Q. Zhu, "Coastal Winds from NOAA Near Real-Time SCATSAT-1 Scatterometer Processor," *OCEANS 2021: San Diego – Porto*, San Diego, CA, USA, 2021, pp. 1-5, doi: 10.23919/OCEANS44145.2021.9705706.

> REPLACE THIS LINE WITH YOUR MANUSCRIPT ID NUMBER (DOUBLE-CLICK HERE TO EDIT) <

High-Resolution Coastal Winds from the NOAA Near Real-Time ASCAT Processor

Seubson Soisuvarn, Zorana Jelenak, Paul S. Chang, Qi Zhu, and Casey G. Shoup

***Abstract*—The NOAA near real-time operational ASCAT ocean surface wind vectors are produced at 12.5 and 25 km swath grid resolutions. To avoid land contamination due to the relatively large footprint size, the wind data in the inner most coastal regions (~15 - 25 km from the coast) are excluded from the final product. To obtain more retrievals in the coastal regions we utilize measurements containing up to 50% land contribution ratio and employ a combination of the enhanced resolution processing technique and a coastal normalized radar cross section correction method to achieve accurate wind retrievals to within ~1.0 - 2.5 km of the coast. The backscatter correction is implemented for each ASCAT coastal zone measurement. The mean and standard deviation of the land contribution for each measurement is determined, and then the land backscatter contribution is subtracted out from the actual measurement through an iteration method to estimate the ocean-only signal. An ocean calibration of the enhanced resolution backscatter was implemented before the wind retrieval step to improve the accuracy. Finally, a land contribution ratio ranking is implemented after the wind retrieval to further remove the remaining land contamination residuals. Additional quality control is also developed. The high-resolution coastal winds from ASCAT are validated against a variety of other independent wind measurements. The results are then presented and discussed.**

***Index Terms*—ASCAT, Scatterometer, High-Resolution, Coastal Winds.**

I. INTRODUCTION

THE coastal sea surface wind field information is important for a number of applications, such as marine weather forecasting, coastal management, fisheries management, ice motion, recreational boating, food and oil production, and energy harvesting. The oceanic vertical motion induced by winds and currents is also important to biology and biogeochemistry within the ocean column. The Advanced SCATterometer (ASCAT) is capable of providing this important wind information over the global oceans. The

the MetOp-A satellite, so called the ASCAT-A, on 19 October 2006 and was decommissioned on 15 November 2021. The follow-on ASCAT-B and -C were launched on MetOp-B and MetOp-C on 17 September 2012 and 7 November 2018, respectively and they are still operational at the time of this writing. ASCAT, a microwave radar instrument, operates at a frequency of 5.255 GHz (C-band). It transmits and receives radar pulses using two sets of three vertically polarized fixed fan-beam antennas. The return radar backscatter power is used to calculate the normalized radar cross-section (NRCS) or sigma0 (σ^0) measurements used in the wind retrieval algorithm. The antennas illuminate fan beams looking ±45° forward (fore beams), ±90° sideway (mid beams) and ±135° backward (aft beams) with respect to the satellite's flight direction to create a measurement swath of approximately 550-km on each side for the satellite ground track with a 700 km gap between the two swaths. The illuminated antenna footprint of the fore and aft beams span incidence angles between 37°-64°; while the mid beam footprint spans incidence angles between 27°-52° with the shape and size of the spatial response function (SRF) of the individual NRCS samples as defined in [2] [3]. As the satellite moves forward, a triplet of sigma0 measurement within a wind vector cell (WVC) from the fore, mid and aft beams are used to retrieve the ocean surface wind vector through an empirically derived Geophysical Model Function (GMF) [4] [5] [6] [7]. The wind retrievals are derived for each WVC (typically at 12.5 km or 25 km sampling) along and across the swaths.

NOAA has operationally produced near real-time global ASCAT ocean surface wind vector products at 12.5 km and 25 km swath grid resolutions [6] since 2007. While extremely valuable to NOAA's user community [8], the coverage of these data products are quite limited in the coastal area because the relatively coarse spatial resolution required a conservative land mask to avoid land contamination in the coastal zone grid cells. This results in no wind data within ~15 - 25 km of the coast. To

S. Soisuvarn, Z. Jelenak, P. S. Chang, Q. Zhu and C. G. Shoup, "High-Resolution Coastal Winds From the NOAA Near Real-Time ASCAT Processor," in *IEEE Transactions on Geoscience and Remote Sensing*, vol. 61, pp. 1-12, 2023, Art no. 5208612, doi: 10.1109/TGRS.2023.3279764.